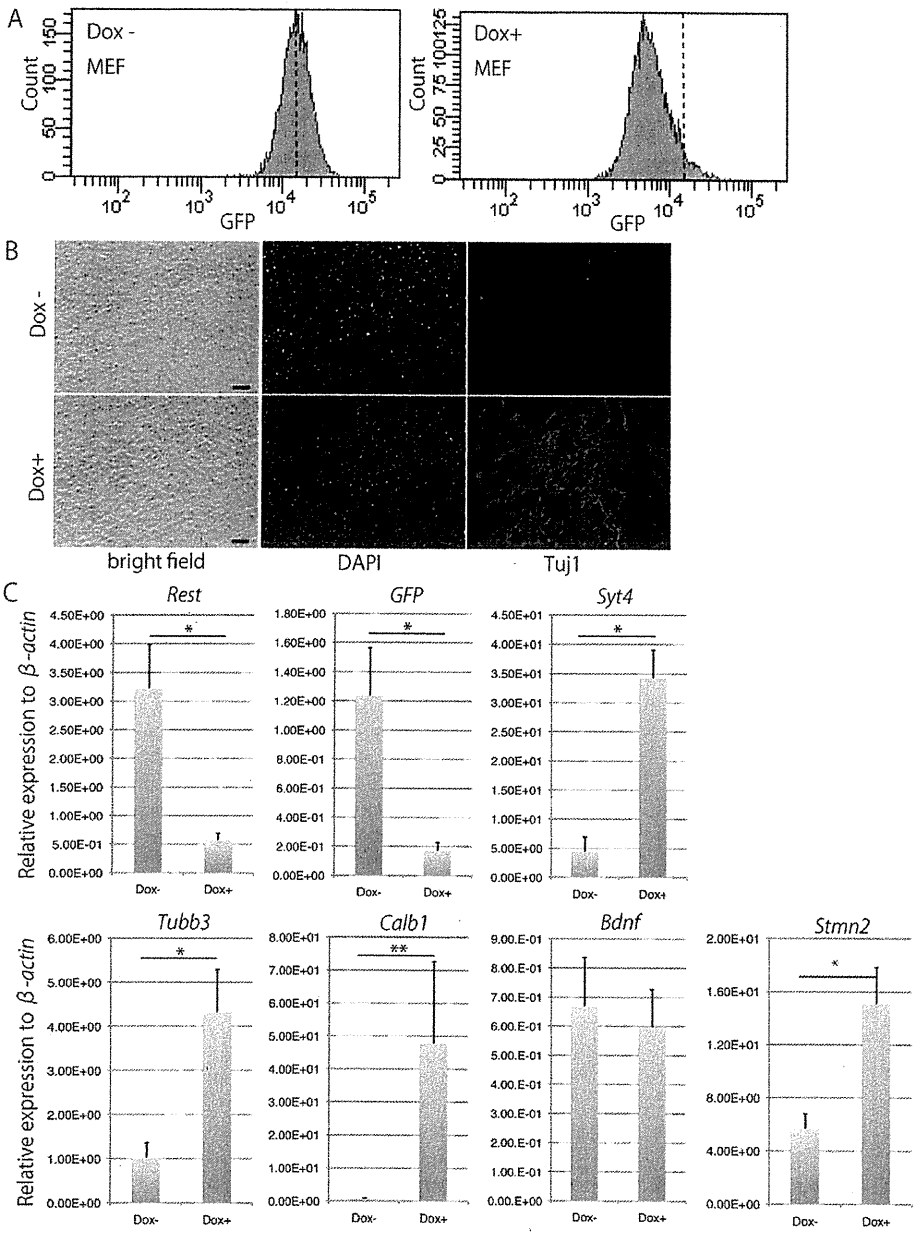

Fig. 2. The conditional deletion of *Rest* in mouse embryonic fibroblasts leads to derepression of Rest target genes. (**A**) FACS analysis revealed a decreased signal for GFP fluorescence in doxycycline-treated mouse embryonic fibroblasts (MEFs) 7 days after seeding of the MEFs. The dashed line indicates the GFP signal at the peak of the histogram of the control cells for comparison. (**B**) The conditional deletion of *Rest* in MEFs resulted in an increased number of Tuj1-positive cells in vitro. Tuj1 expression was also observed in some postmitotic neuronal cells with long axons, which were likely to be contaminating neuronal cells present in the MEF culture. Scale bars: 100 μm. (**C**) Transcript levels of *Rest*, *GFP* and Rest target genes. The expression levels of the Rest target genes *Syt4*, *Tubb3*, *Calb1* and *Stmn2* were significantly upregulated, whereas the expression levels of *Rest* and *GFP* were downregulated after *Rest* ablation in MEFs. No significant change was detectable in the *Bdnf* expression level. Transcript levels were normalized to β-actin levels. The data are presented as average values with s.d. of nine independent samples. *, $P<0.00001$; **, $P<0.0005$.

In vitro ablation of *Rest* in neuronal progenitor cells

Rest is downregulated in the brain as gestation progresses (Ballas et al., 2005). We first examined the expression of *Rest* in the developing mouse brain. The conditional KO alleles contain IRES-*GFP* sequences at the 3′ UTR of the *Rest* gene, which enable us to detect the expression and distribution of *Rest* by the GFP signals. By analyzing GFP expression, we confirmed that cells in the brain at E13.5 actually express the *Rest* gene (Fig. 3A).

In order to investigate the effect of genetic ablation of *Rest* during neurogenesis in vitro, we generated neurospheres from the brains of E13.5 *Rest* conditional KO embryos carrying the doxycycline-inducible *Cre* alleles. The primary neurospheres were passaged to form secondary neurospheres. Doxycycline was administered for 3 days starting 1 day after the passage of the primary neurospheres (passage 1). When we measured the number of secondary neurospheres in order to compare the formation of neurospheres in the presence and absence of doxycycline, the number of neurosphere cells was not significantly different 1 week after passage, regardless of doxycycline exposure (Fig. 3B). By contrast, the number of cells constituting the neurospheres exposed to doxycycline was significantly decreased after long-term culture of the neurospheres (Fig. 3C), suggesting that the ablation of *Rest* inhibited the growth of the neurospheres. Since a recent study demonstrated that *Rest* ablation in cultured neurosphere cells actually results in decreased proliferation (Gao et al., 2011), the decreased proliferative activity might be responsible for the decreased number of cultured cells upon doxycycline treatment in vitro.

We next cultured *Rest* conditional KO neurospheres (*Rest*$^{2lox/2lox}$; *Rosa26::rtTA*; *Col1a1::tetO-Cre*) under differentiation conditions. To examine the effects of *Rest* ablation on neuronal differentiation, the

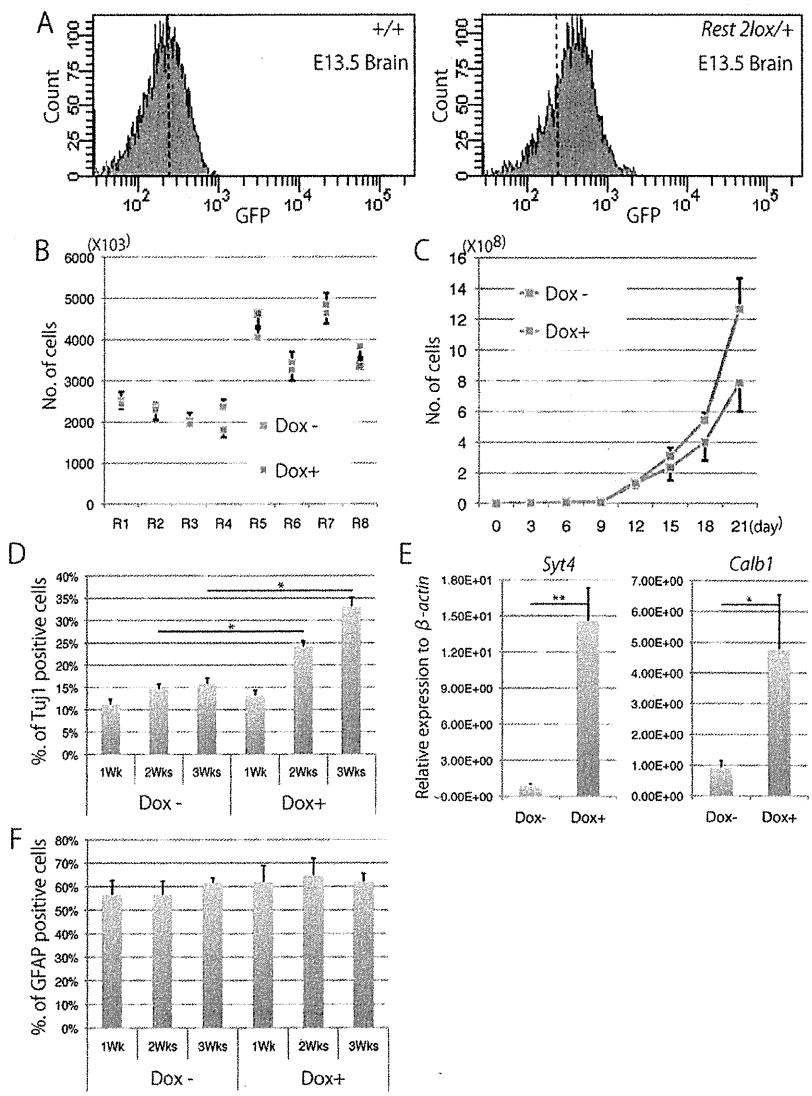

Fig. 3. *Rest* ablation in in vitro cultured neuronal cells. (**A**) FACS analysis for GFP fluorescence. The $Rest^{2lox}$ allele contains IRES-GFP sequences at the 3'UTR of the *Rest* gene, which allows visualization of *Rest* expression via GFP signals. Cells in the E13.5 mouse brain expressed GFP, suggesting that *Rest* is expressed in the developing brain. Dashed line represents the GFP signal at the peak of the histogram of the control cells for comparison. (**B**) The number of neurosphere cells in the presence and absence of doxycycline. The data are presented as the mean number of neurosphere cells in eight independent experiments (R1-R8). Error bars indicate s.d. (**C**) The number of cells constituting neurospheres in the presence and absence of doxycycline. Doxycycline-treated neurospheres grew more slowly than control neurospheres. Error bars indicate s.d. (**D**) The percentage of Tuj1-positive cells among total differentiated neurosphere cells after genetic deletion of *Rest*. The number of Tuj1-positive cells among total cells was significantly increased after *Rest* ablation. The data are presented as average values with s.d. of three independent samples. (**E**) The expression of *Syt4* and *Calb1* is derepressed after *Rest* ablation in neurosphere-derived differentiated cells. Transcript levels were normalized to β-actin levels. The data are presented as average values with s.d. of six independent samples. (**F**) The percentage of Gfap-positive cells among total differentiated neurosphere cells after genetic deletion of *Rest*. The number of Gfap-positive cells among total cells did not change following genetic ablation of *Rest*. The data are presented as average values with s.d. of three independent samples. *, $P<0.001$; **, $P<0.00005$.

doxycycline treatment was started 1 day after seeding the neurospheres in adherent culture, and the cells were treated with doxycycline for an additional 3 days. The adherent spheres were stained with anti-Tuj1 and anti-Gfap antibodies 1, 2 and 3 weeks after doxycycline exposure (Fig. 3D and supplementary material Fig. S5) and we counted the number of Tuj1-positive or Gfap-positive cells and DAPI-positive (total) nuclei in three independent areas of 1.5 mm^2 to calculate the proportion of Tuj1-positive or Gfap-positive cells. The doxycycline-treated cells contained a significantly increased percentage of Tuj1-positive cells among total cells than the control non-treated cells after 2 and 3 weeks of the treatment (Fig. 3D). In addition, a real-time PCR analysis revealed that the expression levels of *Syt4* and *Calb1* increased in the neurosphere adherent culture after genetic ablation of *Rest* (Fig. 3E). By contrast, the percentage of Gfap-positive glial cells among total cells was not altered (Fig. 3F), suggesting that ablation of *Rest* does not have a significant effect on glial differentiation in vitro in this experimental condition.

Because the Tuj1 and Gfap double-negative cells in the adherent spheres decreased after doxycycline treatment, *Rest* ablation may induce Tuj1 expression in such Tuj1 and Gfap double-negative cells. Immunocytochemical analysis of doxycycline-treated neurosphere cells revealed that a subset of non-neuron-like cells expresses Tuj1 and/or calbindin, whereas non-neuron-like cells in the control neurospheres did not express these markers (supplementary material Fig. S6A,B). Consistent with a previous study (Gao et al., 2011), we observed a small number of cells that express both Tuj1 and Gfap, suggesting the misexpression of Rest target genes (supplementary material Fig. S6C). Collectively, these results suggest that derepression of Rest target genes occurred in the adherent neurosphere cells upon *Rest* ablation, and that this derepression might play a role in the promotion of neuronal differentiation.

The in vivo effects of *Rest* ablation on gene expressions in non-neuronal and neuronal cells of the developing embryo

In the E13.5 mouse embryo the expression level of *Rest* in the limb was higher than that in the brain (supplementary material Fig. S7). By contrast, the expression level of Rest target genes was higher in the brain than in the limb (supplementary material Fig. S7).

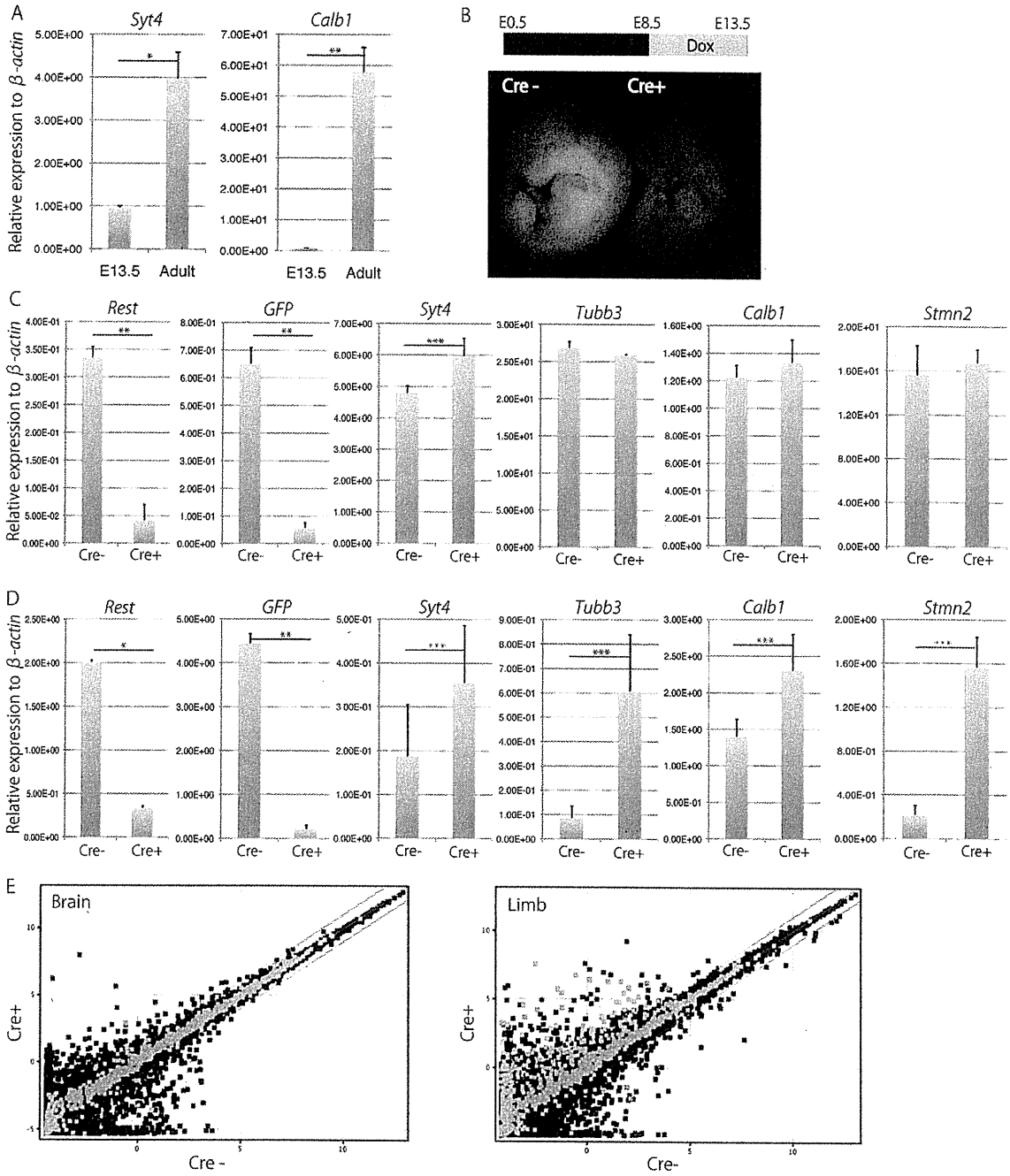

Fig. 4. In vivo genetic ablation of *Rest* in developing embryos. (**A**) Neuronal gene expression levels in the brains of E13.5 embryos and adult mice. The expression of *Syt4* and *Calb1* was significantly higher in the adult brain, suggesting that Rest neuronal target genes are still repressed in the E13.5 brain. The transcript levels were normalized to β-actin. The data are presented as average values with s.d. of six independent samples. (**B**) The experimental protocol for recombination of the *Rest* alleles in vivo. Pregnant mice with *Rest* conditional KO embryos were treated with doxycycline for 5 days, and embryos were sacrificed at E13.5. GFP fluorescence was decreased in embryos with the *tetO-Cre* allele, as compared with control embryos without the *tetO-Cre* allele. (**C**) The in vivo expression of Rest target genes in the brain. Although the expression levels of *Rest* and *GFP* were significantly downregulated, the expression levels of most Rest target genes were not derepressed in the brains of *Cre+* embryos. Transcript levels were normalized to β-actin. The data are presented as average values with s.d. of four independent samples. (**D**) The expression of Rest target genes in the peripheral tissues (limb) in vivo. The expression of *Syt4*, *Tubb3*, *Calb1* and *Stmn2* was derepressed after genetic deletion of *Rest*. Transcript levels were normalized to β-actin. The data are presented as average values with s.d. of four independent samples. (**E**) A microarray analysis of E13.5 brain and non-neuronal (limb) tissue after genetic ablation of *Rest*. Rest binding genes in neuronal stem cells (Johnson et al., 2008) are shown as green dots. Rest target genes were significantly upregulated in the *Rest*-deleted non-neuronal tissue (limb). By contrast, the derepression of Rest target genes in the brain was not observed following genetic ablation of *Rest*. *, $P<0.01$; **, $P<0.005$; ***, $P<0.05$.

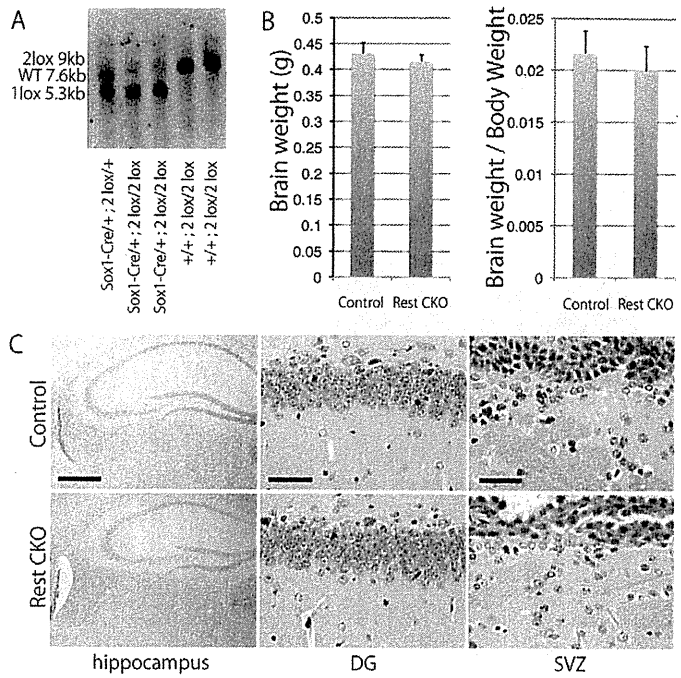

Fig. 5. The effect of *Rest* ablation on neurogenesis in vivo. (**A**) Southern blot analysis revealed that *Rest* conditional KO (2lox, 9kb) alleles in the adult brain with the *Sox1-Cre* allele recombined to form KO (1lox, 5.3kb) alleles. The wild-type (WT) allele appeared at 7.6 kb. (**B**) Comparison of brain weight and the ratio of brain weight to body weight in 8-week-old *Rest* conditional KO and control mice. Neither the brain weight nor the ratio was significantly different in *Sox1-Cre/+*; $Rest^{2lox/2lox}$ adult mice compared with control littermates. (**C**) The histology of adult brains from *Sox1-Cre/+*; $Rest^{2lox/2lox}$ mice (8 weeks of age). No histological differences were detectable in the dentate gyrus (DG, middle) of the hippocampus (left) and subventricular zone (SVZ, right) of the brains from *Sox1-Cre/+*; $Rest^{2lox/2lox}$ versus control adult mice by HE staining. Scale bars: 50 μm in DG and SVZ; 500 μm in hippocampus.

However, the expression levels of *Syt4* and *Calb1* in the E13.5 brain were significantly lower than those in the adult brain (Fig. 4A). These observations are consistent with the hypothesis that the expression of Rest target genes is still repressed in the E13.5 brain in vivo. Since our in vitro experiments revealed that the genetic ablation of *Rest* results in the increased expression of Rest target genes in both non-neuronal and neuronal cells, we next tried to dissect the effects of *Rest* ablation on the non-neuronal and neuronal cells in vivo using embryos with floxed *Rest* genes and doxycycline-inducible *Cre* alleles. The *Rest* conditional KO embryos were treated with doxycycline in utero (E8.5-13.5) to induce Cre-mediated recombination in both non-neuronal and neuronal cells, and the mice were sacrificed at E13.5 (Fig. 4B). In accordance with the recombination, E13.5 embryos with a *tetO-Cre* allele had decreased signals for GFP when compared with embryos without a *tetO-Cre* allele (Fig. 4B). We also collected the brains and limbs from *Rest*-deleted embryos and their control littermates without the *tetO-Cre* allele. Consistent with the decreased GFP signals, real-time RT-PCR analysis revealed that the expression of *Rest* was significantly downregulated in both the brain and limbs from embryos with a *tetO-Cre* allele compared with those from control littermates (Fig. 4C,D).

Similar to the results obtained in vitro, we detected a significant increase in the expression of *Syt4*, *Tubb3*, *Calb1* and *Stmn2* in the limbs of embryos with the *tetO-Cre* allele (Fig. 4D). By contrast, the expression level of *Tubb3*, *Calb1* and *Stmn2* in the brains of E13.5 embryos with a *tetO-Cre* allele remained repressed, whereas the expression levels of *Rest* and *GFP* itself were downregulated in the same samples (Fig. 4C). Although the expression of *Syt4* was slightly upregulated in the brain of embryos with a *tetO-Cre* allele (Fig. 4C), the effect was only modest when compared with the levels in the adult brain (Fig. 4A). Immunohistochemical analysis confirmed that there was no alteration in the expression pattern of Tuj1 in the E13.5 brain of embryos with a *tetO-Cre* allele (supplementary material Fig. S8A). We also examined the expression of Rest target genes in the brain or tail of E16.5 embryos with a *tetO-Cre* allele, and found no altered expression levels of these genes in brains, whereas a significant increase in the expression of *Syt4*, *Calb1* and *Stmn2* was observed in the tail (supplementary material Fig. S8B). These results indicate that the Rest target genes are specifically derepressed in non-neuronal cells outside of the brain by the genetic ablation of *Rest* in vivo.

We next performed a microarray analysis to determine the changes in gene expression after genetic deletion of *Rest* in E13.5 brain and limb in vivo. Consistent with the results of the real-time RT-PCR analysis, Rest target genes were significantly upregulated in the *Rest*-deleted limb tissue (Fig. 4E; genes interacting with Rest in ESCs and NPCs are represented by green dots) (Johnson et al., 2008). However, the derepression in the limb tissues (upregulated more than 2-fold after *Rest* ablation) was observed in only a subset of the genes with a Rest binding site (27% of the genes; Fig. 4E, limb), suggesting gene-specific derepression. By contrast, only 2% of the genes with a Rest binding site were upregulated more than 2-fold in the brain, suggesting that the derepression only occurs at a minority of Rest target genes after the genetic ablation of *Rest* (Fig. 4E, brain).

In vivo ablation of *Rest* in progenitor cells of the developing brain

Sox1 was shown to be one of the earliest transcription factors expressed in ectoderm cells committed to a neural fate (Pevny et al., 1998; Takashima et al., 2007). The expression of *Sox1* starts at E7.5-8.5 in the neural tube (Takashima et al., 2007). We used a *Sox1-Cre* allele (Takashima et al., 2007) ($Rest^{2lox/2lox}$; *Sox1-Cre/+*) to excise the floxed *Rest* genes in early progenitor cells of the developing mouse brain in vivo. The brains from *Rest* conditional KO mice carrying the *Sox1-Cre* allele ($Rest^{2lox/2lox}$; *Sox1-Cre/+*) and control littermates ($Rest2^{lox/2lox}$) were collected at E13.5, E16.5 and postnatal day (P) 0 and the expression levels of Rest target genes were compared by real-time RT-PCR. The brains from

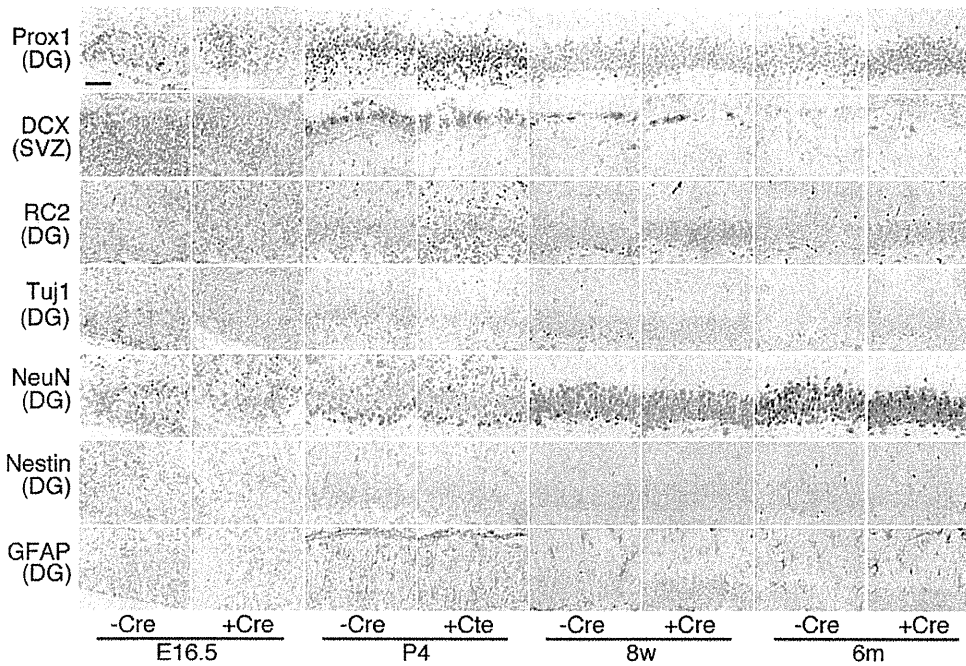

Fig. 6. Sequential immunohistochemical analysis for Prox1, Dcx, RC2, Tuj1, NeuN, nestin and Gfap. Brains at E16.5, P4, 8 weeks (8w) and 6 months (6m) of *Rest*-deficient and control mice were analyzed. DG, dentate gyrus; SVZ, subventricular zone. Scale bar: 50 μm.

embryos carrying *Sox1-Cre* had significantly lower levels of both *Rest* and *GFP* expression at all time points, reflecting the genetic ablation of *Rest* (supplementary material Fig. S9). However, consistent with the results in the experiments using doxycycline-inducible *Cre* mice, the expression levels of Rest target genes such as *Syt4*, *Tubb3*, *Calb1*, *Bdnf* and *Stmn2* (except for *Stmn2* at E13.5) were not significantly increased in the brains of developing embryos with the *Sox1-Cre* allele (supplementary material Fig. S9). These results confirm that the conditional deletion of *Rest* does not substantially affect the expression of Rest neuronal target genes in the developing brain.

Rest ablation during adult neurogenesis in vivo

To further examine the function of *Rest* in the maintenance of neurogenesis in adult brain tissue, we analyzed the brains of adult *Rest* conditional KO mice carrying the *Sox1-Cre* allele. Contrary to our expectation, the *Rest* conditional KO mice carrying the *Sox1-Cre* allele were apparently normal and grew into adults. These mice were viable for more than 1.5 years and were fertile. A Southern blot analysis confirmed that the brains of mice with the *Sox1-Cre* allele had lost the floxed *Rest* genes (Fig. 5A). Despite the lack of *Rest* throughout the entire brain tissue (Fig. 5A), brain weight at 8 weeks of age was not significantly different between the mice with and without the *Sox1-Cre* allele (Fig. 5B).

Next, we examined the histology of the brains of mice with and without the *Sox1-Cre* allele at different developmental stages and ages (E16.5, P0, P4, P7, P10, 4 weeks, 8 weeks, 10 weeks, 6 months and 9 months of age). However, we did not find any histological differences in the brains, including in the subgranular zone (SGZ) of the hippocampal dentate gyrus and the subventricular zone (SVZ), where NSCs and NPCs reside and generate new neurons and glia (Fig. 5C) (Gage, 2002). We further performed immunohistochemical staining to examine the expression of various markers, including Prox1, Dcx, RC2, Tuj1, NeuN (Rbfox3 – Mouse Genome Informatics), nestin and Gfap at various time points (E16.5, P4, 8 weeks and 6 months) in the *Rest*-deficient and control brains. Prox1, Dcx and RC2 were used as markers for intermediate progenitor cells, immature neuronal cells and radial glial cells, respectively (Gao et al., 2011; Misson et al., 1988). Importantly, we did not observe any difference in the staining patterns of these markers between *Rest*-deficient and control brains (Fig. 6). We also confirmed that nestin-positive cells and Gfap-positive cells did not express Tuj1 in *Rest*-deficient brain, suggesting that misexpression of Tuj1 does not occur in the *Rest*-deficient cells in vivo (supplementary material Figs S10, S11). Although a recent study showed that acute *Rest* ablation in mice leads to a decreased number of Prox1-positive cells at SGZ regions, we did not observe any significant differences in the number of Prox1-positive cells, even in 9-month-old mice (supplementary material Fig. S12).

In order to examine the effect of *Rest* ablation on the maintenance of adult NSCs, we compared the numbers of BrdU-labeled cells in the SVZ of the adult brain of the *Rest* conditional KO mice carrying the *Sox1-Cre* allele with those of control littermates (Doetsch et al., 2002; Lendahl et al., 1990). BrdU was administered as a daily intraperitoneal injection of 50 mg/kg body weight for 12 days starting at the age of 8 weeks, and the brains were fixed 1 day after the last injection as described previously (Shi et al., 2004). We did not find any significant difference in the number of BrdU-positive cells in the SVZ of these mice (Fig. 7A). We also confirmed co-localization of BrdU-positive cells and those positive for Dcx, a marker for premature neuronal cells, in the SVZ of *Rest*-deficient mice (Fig. 7B), suggesting that adult neurogenesis occurs in these mice. In addition, the localization and the number of differentiated NeuN-positive cells in the adult mouse brain did not differ in the presence or absence of the intact *Rest* gene (Fig.

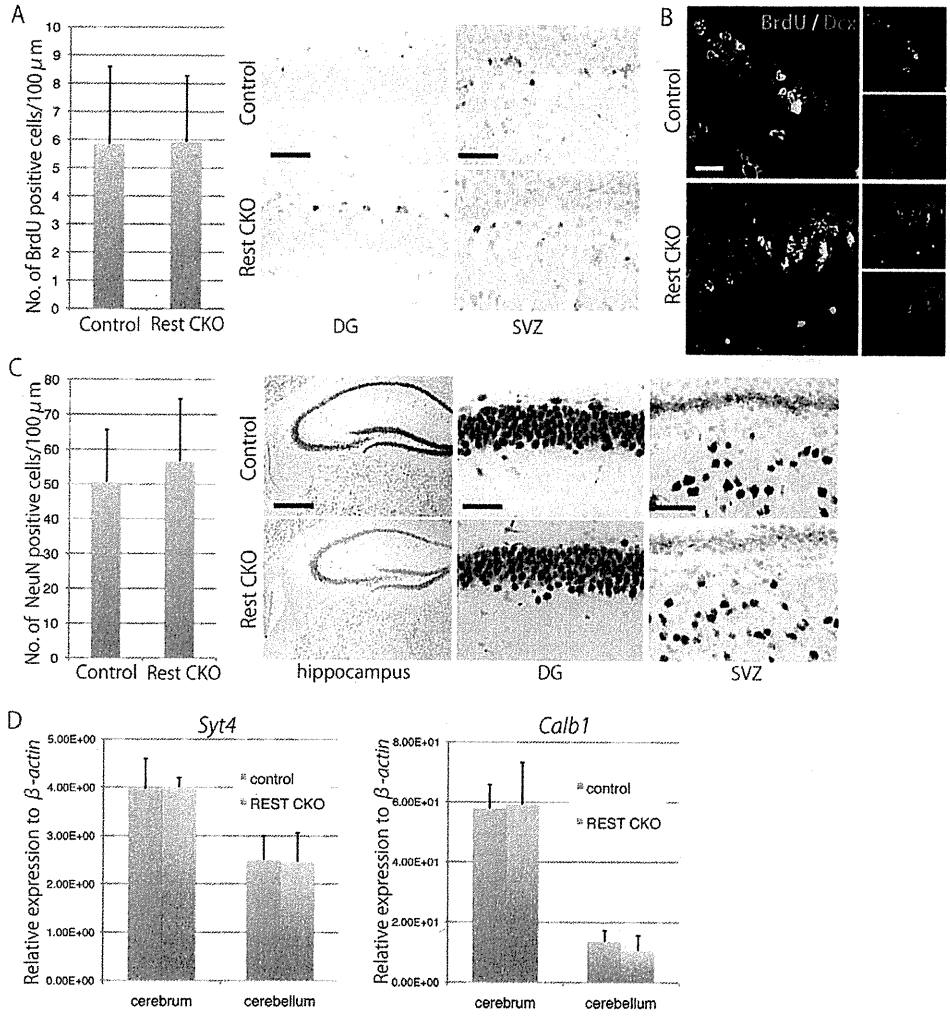

Fig. 7. Adult neurogenesis in *Rest*-deficient brains in vivo. (**A**) Immunohistochemical analysis of BrdU-positive proliferating cells in the adult brain (10 weeks of age). There were no differences in the distribution of BrdU-positive cells in DG and SVZ regardless of genotype. The number of BrdU-positive cells/length of cerebral ventricle in the brains of *Sox1-Cre/+*; $Rest^{2lox/2lox}$ mice was not altered compared with that of their control littermates. (**B**) Immunohistochemical staining for BrdU (green) and Dcx (red) double-positive cells in the SVZ of brain from *Sox1-Cre/+*; $Rest^{2lox/2lox}$ mice and control littermates at 10 weeks of age. (**C**) Immunohistochemical staining for NeuN in the DG of the hippocampus and SVZ of brains from *Sox1-Cre/+*; $Rest^{2lox/2lox}$ mice and their control littermates at 8 weeks of age. (**D**) The expression of Rest target genes in the adult mouse brain at 8 weeks of age. The expression of *Syt4* and *Calb1* was unchanged in the cerebrum and cerebellum of *Sox1-Cre/+*; $Rest^{2lox/2lox}$ mice. Transcript levels were normalized to β-actin levels. The data are presented as average values with s.d. of six independent samples. Scale bars: 50 μm in DG and SVZ; 500 μm in hippocampus; 20 μm in B.

7C). A real-time RT-PCR analysis revealed that the expression of *Syt4* and *Calb1* was not altered in the adult brains lacking the CoRest binding site of *Rest* (Fig. 7D).

These results indicate that *Rest* is not required for brain development and suggest that genetic ablation of *Rest* during the initial stage of neural development does not cause any detectable abnormality in adult neurogenesis in vivo.

DISCUSSION

Differentiation of neuronal progenitors to mature neurons proceeds with loss of the Rest repressor complex from the RE1 site of neuronal genes, which is accompanied by increased expression of the target genes (Ballas et al., 2005). In the present study, using *Rest* conditional KO mice we confirmed that *Rest* plays a role in the repression of Rest neuronal target genes in in vitro cultured neuronal progenitor cells to inhibit terminal differentiation. By contrast, genetic ablation of *Rest* in the whole brain in vivo does not result in altered expression of target genes. Furthermore, mice lacking *Rest* in the brain are apparently normal and grow into adults. These findings suggest that, in contrast to the repressive role of *Rest* in in vitro cultured neuronal cells, *Rest* is dispensable for embryonic neurogenesis in vivo.

The unsolved question is why derepression of Rest target genes after *Rest* ablation can be detected in in vitro cultured neuronal cells but not in developing brain tissue in vivo. It has been demonstrated that neuronal progenitor cells are competent for extrinsic signals involved in the specification of cell fate during neurogenesis (Edlund and Jessell, 1999). Our findings suggest that the local environment in the brain, which consists of multiple cell types, is likely to provide complementary regulatory mechanisms for the proper intrinsic regulation of neuronal genes in vivo. It is noteworthy that, in the non-neuronal cells outside of the brain, the derepression of Rest target genes was observed not only in vitro but also in vivo. These findings suggest that the brain-specific environment is important for the complementary repression of Rest target genes in the absence of *Rest*.

Epigenetic mechanisms serve as important interfaces between gene expression and the environment (Jaenisch and Bird, 2003). Given that Rest exerts its repressive effects in conjunction with epigenetic modifiers (Ballas et al., 2005; Naruse et al., 1999; You et al., 2001), it is possible that extrinsic niche signals in the brain compensate for the lack of Rest through epigenetic regulatory mechanisms. Consistent with this hypothesis, we could not detect

any differences in the staining pattern of histone H3K27me3, a mark of epigenetic silencing, between *Rest* wild-type and *Rest*-deficient brains in vivo (data not shown).

Another study indicated that MeCP2 and other co-repressors remained on the Rest target promoters even after loss of Rest from the RE1 site, suggesting that Rest co-repressors might be involved in the additional regulatory mechanisms that are responsible for repressing the expression of neuronal genes in neuronal cells in the absence of Rest (Ballas et al., 2005). It is possible that such factors specifically compensate for the effect of *Rest* ablation in the repression of Rest neuronal target genes during embryonic neurogenesis in vivo. It is also possible that transcriptional activators might be required for the derepression of Rest target genes in the developing brain. In this context, the decreased levels of transcriptional activation might maintain the proper expression levels of Rest target genes in *Rest*-deficient brains in vivo.

A recent study by Gao et al. demonstrated that the acute deletion of *Rest* in the adult dentate gyrus (DG) leads to a decreased number of Prox1-positive DG cells (Gao et al., 2011). However, in the present study, we did not observe any significant differences in the number of Prox1-positive DG cells upon *Rest* ablation, even in 9-month-old mice. A possible explanation for the discrepancy is that the acute deletion of *Rest* in the adult DG cannot activate the compensatory mechanisms, resulting in premature differentiation of adult NSCs, whereas its deletion at the early embryonic stage, as performed in this experiment, activates the complementary machinery that masks Rest function at adult stages. Therefore, further experiments are still required to determine the role of Rest in the maintenance of adult NSCs in vivo.

The expression of Rest target genes in MEFs/TTFs is upregulated upon the loss of *Rest*, suggesting that Rest is involved in the active repression of neuronal genes in non-neuronal cells outside of the brain. However, we found that *Bdnf*, which contains RE1 sites and is repressed by Rest in ESCs (Yamada et al., 2010), was not derepressed after the deletion of *Rest* in MEFs/TTFs. As reported in a previous study (Chen et al., 1998), these findings suggest that there is cell type specificity of Rest-mediated gene silencing. In addition, a microarray analysis revealed that only a subset of genes with a Rest binding site (27%) is derepressed by more than 2-fold following genetic ablation of *Rest* in non-neuronal tissues. In addition to the cell type-specific repression, these findings suggest that there is gene-specific repression by Rest (Chen et al., 1998). Since epigenetic silencing occurs through multiple modifications, including DNA methylation and histone modifications (Jaenisch and Bird, 2003; Lunyak et al., 2002; Martinowich et al., 2003), *Rest* deletion alone might not be sufficient to reactivate the silenced locus once silencing, involving multiple epigenetic modifications, has been completed. It is also possible that the cell type- and gene-specific activity of transcriptional activators is responsible for such different responses to *Rest* deletion.

The impaired interaction of Rest with its target genes has been reported in various neurological and neurodegenerative diseases. Although we found that mice lacking the CoRest binding site of *Rest* in the brain had no gross anatomical abnormalities even upon reaching adulthood, it is possible that more detailed analyses might highlight behavioral abnormalities in the *Rest* KO mice. In this context, these mice might be useful in investigation of the role of altered Rest interactions in neurological and neurodegenerative diseases. It would also be interesting to examine the functional alterations of *Rest*-deficient neuronal cells in vivo, which eventually might uncover the pathogenesis of such diseases.

In summary, we have generated *Rest* conditional KO mice and examined the effects of *Rest* ablation in neuronal and non-neuronal cells in vitro and in vivo. We showed that, in contrast to the role of *Rest* in the repression of Rest target genes in in vitro cultured neuronal cells, as well as in non-neuronal cells outside of the brain, the CoRest binding site of *Rest* is dispensable for embryonic neurogenesis in vivo.

Acknowledgements
We thank Kyoko Takahashi and Ayako Suga for technical assistance; Caroline Beard for the *Col1a-tetOP-cre* allele; and Shinichi Nishikawa for *Sox1-Cre* mice.

Funding
This study was supported by grants from the Ministry of Education, Culture, Sports, Science and Technology of Japan; Precursory Research for Embryonic Science and Technology (PRESTO); and the Ministry of Health, Labour and Welfare of Japan.

Competing interests statement
The authors declare no competing financial interests.

Supplementary material
Supplementary material available online at
http://dev.biologists.org/lookup/suppl/doi:10.1242/dev.072272/-/DC1

References

Abrajano, J. J., Qureshi, I. A., Gokhan, S., Zheng, D., Bergman, A. and Mehler, M. F. (2009). Differential deployment of REST and CoREST promotes glial subtype specification and oligodendrocyte lineage maturation. *PLoS ONE* **4**, e7665.

Andres, M. E., Burger, C., Peral-Rubio, M. J., Battaglioli, E., Anderson, M. E., Grimes, J., Dallman, J., Ballas, N. and Mandel, G. (1999). CoREST: a functional corepressor required for regulation of neural-specific gene expression. *Proc. Natl. Acad. Sci. USA* **96**, 9873-9878.

Ballas, N., Battaglioli, E., Atouf, F., Andres, M. E., Chenoweth, J., Anderson, M. E., Burger, C., Moniwa, M., Davie, J. R., Bowers, W. J. et al. (2001). Regulation of neuronal traits by a novel transcriptional complex. *Neuron* **31**, 353-365.

Ballas, N., Grunseich, C., Lu, D. D., Speh, J. C. and Mandel, G. (2005). REST and its corepressors mediate plasticity of neuronal gene chromatin throughout neurogenesis. *Cell* **121**, 645-657.

Bassuk, A. G., Wallace, R. H., Buhr, A., Buller, A. R., Afawi, Z., Shimojo, M., Miyata, S., Chen, S., Gonzalez-Alegre, P., Griesbach, H. L. et al. (2008). A homozygous mutation in human PRICKLE1 causes an autosomal-recessive progressive myoclonus epilepsy-ataxia syndrome. *Am. J. Hum. Genet.* **83**, 572-581.

Beard, C., Hochedlinger, K., Plath, K., Wutz, A. and Jaenisch, R. (2006). Efficient method to generate single-copy transgenic mice by site-specific integration in embryonic stem cells. *Genesis* **44**, 23-28.

Bruce, A. W., Donaldson, I. J., Wood, I. C., Yerbury, S. A., Sadowski, M. I., Chapman, M., Gottgens, B. and Buckley, N. J. (2004). Genome-wide analysis of repressor element 1 silencing transcription factor/neuron-restrictive silencing factor (REST/NRSF) target genes. *Proc. Natl. Acad. Sci. USA* **101**, 10458-10463.

Canzonetta, C., Mulligan, C., Deutsch, S., Ruf, S., O'Doherty, A., Lyle, R., Borel, C., Lin-Marq, N., Delom, F., Groet, J. et al. (2008). DYRK1A-dosage imbalance perturbs NRSF/REST levels, deregulating pluripotency and embryonic stem cell fate in Down syndrome. *Am. J. Hum. Genet.* **83**, 388-400.

Chen, Z. F., Paquette, A. J. and Anderson, D. J. (1998). NRSF/REST is required in vivo for repression of multiple neuronal target genes during embryogenesis. *Nat. Genet.* **20**, 136-142.

Chong, J. A., Tapia-Ramirez, J., Kim, S., Toledo-Aral, J. J., Zheng, Y., Boutros, M. C., Altshuller, Y. M., Frohman, M. A., Kraner, S. D. and Mandel, G. (1995). REST: a mammalian silencer protein that restricts sodium channel gene expression to neurons. *Cell* **80**, 949-957.

Doetsch, F., Petreanu, L., Caille, I., Garcia-Verdugo, J. M. and Alvarez-Buylla, A. (2002). EGF converts transit-amplifying neurogenic precursors in the adult brain into multipotent stem cells. *Neuron* **36**, 1021-1034.

Edlund, T. and Jessell, T. M. (1999). Progression from extrinsic to intrinsic signaling in cell fate specification: a view from the nervous system. *Cell* **96**, 211-224.

Fink, T. L., Francis, S. H., Beasley, A., Grimes, K. A. and Corbin, J. D. (1999). Expression of an active, monomeric catalytic domain of the cGMP-binding cGMP-specific phosphodiesterase (PDE5). *J. Biol. Chem.* **274**, 34613-34620.

Gage, F. H. (2002). Neurogenesis in the adult brain. *J. Neurosci.* **22**, 612-613.

Gao, Z., Ure, K., Ding, P., Nashaat, M., Yuan, L., Ma, J., Hammer, R. E. and Hsieh, J. (2011). The master negative regulator REST/NRSF controls adult

neurogenesis by restraining the neurogenic program in quiescent stem cells. *J. Neurosci.* **31**, 9772-9786.
Hatano, Y., Yamada, Y., Hata, K., Phutthaphadoong, S., Aoki, H. and Hara, A. (2011). Genetic ablation of a candidate tumor suppressor gene, Rest, does not promote mouse colon carcinogenesis. *Cancer Sci.* **102**, 1659-1664.
Hochedlinger, K., Yamada, Y., Beard, C. and Jaenisch, R. (2005). Ectopic expression of Oct-4 blocks progenitor-cell differentiation and causes dysplasia in epithelial tissues. *Cell* **121**, 465-477.
Jaenisch, R. and Bird, A. (2003). Epigenetic regulation of gene expression: how the genome integrates intrinsic and environmental signals. *Nat. Genet.* **33 Suppl.**, 245-254.
Jepsen, K., Hermanson, O., Onami, T. M., Gleiberman, A. S., Lunyak, V., McEvilly, R. J., Kurokawa, R., Kumar, V., Liu, F., Seto, E. et al. (2000). Combinatorial roles of the nuclear receptor corepressor in transcription and development. *Cell* **102**, 753-763.
Johnson, R., Gamblin, R. J., Ooi, L., Bruce, A. W., Donaldson, I. J., Westhead, D. R., Wood, I. C., Jackson, R. M. and Buckley, N. J. (2006). Identification of the REST regulon reveals extensive transposable element-mediated binding site duplication. *Nucleic Acids Res.* **34**, 3862-3877.
Johnson, R., Teh, C. H., Kunarso, G., Wong, K. Y., Srinivasan, G., Cooper, M. L., Volta, M., Chan, S. S., Lipovich, L., Pollard, S. M. et al. (2008). REST regulates distinct transcriptional networks in embryonic and neural stem cells. *PLoS Biol.* **6**, e256.
Kohyama, J., Sanosaka, T., Tokunaga, A., Takatsuka, E., Tsujimura, K., Okano, H. and Nakashima, K. (2010). BMP-induced REST regulates the establishment and maintenance of astrocytic identity. *J. Cell Biol.* **189**, 159-170.
Lendahl, U., Zimmerman, L. B. and McKay, R. D. (1990). CNS stem cells express a new class of intermediate filament protein. *Cell* **60**, 585-595.
Lepagnol-Bestel, A. M., Zvara, A., Maussion, G., Quignon, F., Ngimbous, B., Ramoz, N., Imbeaud, S., Loe-Mie, Y., Benihoud, K., Agier, N. et al. (2009). DYRK1A interacts with the REST/NRSF-SWI/SNF chromatin remodelling complex to deregulate gene clusters involved in the neuronal phenotypic traits of Down syndrome. *Hum. Mol. Genet.* **18**, 1405-1414.
Lunyak, V. V., Burgess, R., Prefontaine, G. G., Nelson, C., Sze, S. H., Chenoweth, J., Schwartz, P., Pevzner, P. A., Glass, C., Mandel, G. et al. (2002). Corepressor-dependent silencing of chromosomal regions encoding neuronal genes. *Science* **298**, 1747-1752.
Martinowich, K., Hattori, D., Wu, H., Fouse, S., He, F., Hu, Y., Fan, G. and Sun, Y. E. (2003). DNA methylation-related chromatin remodeling in activity-dependent BDNF gene regulation. *Science* **302**, 890-893.
Misson, J. P., Edwards, M. A., Yamamoto, M. and Caviness, V. S., Jr (1988). Identification of radial glial cells within the developing murine central nervous system: studies based upon a new immunohistochemical marker. *Brain Res. Dev. Brain Res.* **44**, 95-108.
Naruse, Y., Aoki, T., Kojima, T. and Mori, N. (1999). Neural restrictive silencer factor recruits mSin3 and histone deacetylase complex to repress neuron-specific target genes. *Proc. Natl. Acad. Sci. USA* **96**, 13691-13696.
Otto, S. J., McCorkle, S. R., Hover, J., Conaco, C., Han, J. J., Impey, S., Yochum, G. S., Dunn, J. J., Goodman, R. H. and Mandel, G. (2007). A new binding motif for the transcriptional repressor REST uncovers large gene networks devoted to neuronal functions. *J. Neurosci.* **27**, 6729-6739.
Pevny, L. H., Sockanathan, S., Placzek, M. and Lovell-Badge, R. (1998). A role for SOX1 in neural determination. *Development* **125**, 1967-1978.
Roopra, A., Qazi, R., Schoenike, B., Daley, T. J. and Morrison, J. F. (2004). Localized domains of G9a-mediated histone methylation are required for silencing of neuronal genes. *Mol. Cell* **14**, 727-738.
Schoenherr, C. J. and Anderson, D. J. (1995). The neuron-restrictive silencer factor (NRSF): a coordinate repressor of multiple neuron-specific genes. *Science* **267**, 1360-1363.
Schoenherr, C. J., Paquette, A. J. and Anderson, D. J. (1996). Identification of potential target genes for the neuron-restrictive silencer factor. *Proc. Natl. Acad. Sci. USA* **93**, 9881-9886.
Shi, Y., Sawada, J., Sui, G., Affar, El B., Whetstine, J. R., Lan, F., Ogawa, H., Luke, M. P. and Nakatani, Y. (2003). Coordinated histone modifications mediated by a CtBP co-repressor complex. *Nature* **422**, 735-738.
Shi, Y., Chichung Lie, D., Taupin, P., Nakashima, K., Ray, J., Yu, R. T., Gage, F. H. and Evans, R. M. (2004). Expression and function of orphan nuclear receptor TLX in adult neural stem cells. *Nature* **427**, 78-83.
Strutz, F., Okada, H., Lo, C. W., Danoff, T., Carone, R. L., Tomaszewski, J. E. and Neilson, E. G. (1995). Identification and characterization of a fibroblast marker: FSP1. *J. Cell Biol.* **130**, 393-405.
Takashima, Y., Era, T., Nakao, K., Kondo, S., Kasuga, M., Smith, A. G. and Nishikawa, S. (2007). Neuroepithelial cells supply an initial transient wave of MSC differentiation. *Cell* **129**, 1377-1388.
Tapia-Ramirez, J., Eggen, B. J., Peral-Rubio, M. J., Toledo-Aral, J. J. and Mandel, G. (1997). A single zinc finger motif in the silencing factor REST represses the neural-specific type II sodium channel promoter. *Proc. Natl. Acad. Sci. USA* **94**, 1177-1182.
Vierbuchen, T., Ostermeier, A., Pang, Z. P., Kokubu, Y., Sudhof, T. C. and Wernig, M. (2010). Direct conversion of fibroblasts to functional neurons by defined factors. *Nature* **463**, 1035-1041.
Yamada, Y., Aoki, H., Kunisada, T. and Hara, A. (2010). Rest promotes the early differentiation of mouse ESCs but is not required for their maintenance. *Cell Stem Cell* **6**, 10-15.
You, A., Tong, J. K., Grozinger, C. M. and Schreiber, S. L. (2001). CoREST is an integral component of the CoREST- human histone deacetylase complex. *Proc. Natl. Acad. Sci. USA* **98**, 1454-1458.
Zuccato, C., Belyaev, N., Conforti, P., Ooi, L., Tartari, M., Papadimou, E., MacDonald, M., Fossale, E., Zeitlin, S., Buckley, N. et al. (2007). Widespread disruption of repressor element-1 silencing transcription factor/neuron-restrictive silencer factor occupancy at its target genes in Huntington's disease. *J. Neurosci.* **27**, 6972-6983.

Cancer Science
The official journal of the Japanese Cancer Association

Genetic ablation of a candidate tumor suppressor gene, *Rest*, does not promote mouse colon carcinogenesis

Yuichiro Hatano,[1] Yasuhiro Yamada,[2,3,5] Kazuya Hata,[1] Suphot Phutthaphadoong,[1] Hitomi Aoki[4] and Akira Hara[1]

[1]Department of Tumor Pathology, Gifu University Graduate School of Medicine, Gifu; [2]PRESTO, Japan Science and Technology Agency, Saitama; [3]Center for iPS Cell Research and Application, Institute for Integrated Cell-Material Sciences, Kyoto University, Kyoto; [4]Department of Tissue and Organ Development, Gifu University Graduate School of Medicine, Gifu, Japan

(Received March 23, 2011/Revised May 30, 2011/Accepted June 7, 2011/Accepted manuscript online June 11, 2011/Article first published online July 21, 2011)

Colon carcinogenesis is a multistage process involving genetic alterations of various tumor suppressor genes and oncogenes. Repressor element 1 silencing factor (*REST*), which was originally discovered as a transcriptional repressor of neuronal genes, plays an important role in neuronal differentiation. In a previous genetic screening for tumor suppressor genes in human cancers, *REST* was identified as a candidate tumor suppressor gene in colorectal carcinogenesis. However, the role of *Rest* in colon carcinogenesis *in vivo* remains unclear because of the embryonic lethal phenotype of the conventional *Rest* knockout mouse. In the present study, we conditionally deleted the *Rest* gene in the intestinal epithelium and investigated the effect of *Rest* ablation in mouse colon tumorigenesis. A conditional ablation of *Rest* in the colonic crypts led to a rapid upregulation of Rest-targeted genes, such as *Syt4*, *Bdnf*, and *Tubb3*, suggesting that Rest actually suppresses the expression of its target genes in the colon. However, *Rest* ablation did not lead to any significant effect on the development of colon tumors in two independent mouse models of colon carcinogenesis. In addition, despite the upregulation of neuronal genes in the colonic crypts, no neuronal differentiation was observed in the colonic crypts and tumors after the *Rest* ablation. These results indicate that the loss of *Rest* expression by itself does not promote the development of colon tumors in mice, and suggest that REST may exert a tumor suppressing activity in conjunction with the additional genetic/epigenetic abnormalities that occur during colon carcinogenesis. (*Cancer Sci* 2011; 102: 1659–1664)

Repressor element 1 silencing factor (REST; also called neuron-restrictive silencing factor [NRSF]) was originally discovered as a transcriptional repressor of a number of neuronal genes.[1,2] REST binds to a conserved 21–23 bp motif known as repressor element 1 within the control regions of target genes, and recruits multiple co-factors through repressor domains to alter epigenetic modifications, leading to the generation of a silencing complex. REST is ubiquitously expressed in non-neuronal cells,[3] and it prevents neuronal gene expression in non-neuronal cells.[4]

A link between *REST* dysfunction and carcinogenesis has been recognized[5–7] in a number of cancers such as prostate cancer,[8] breast cancer,[9–11] small cell lung cancer,[12–16] medulloblastoma,[17–19] and neuroblastoma.[20–23] In an RNAi-based screening for tumor suppressor genes, *REST* was identified as a candidate novel tumor suppressor gene.[24] Consistent with this notion, a *REST* mutation was identified in a colon cancer cell line, DLD-1, and the *REST* locus is deleted in approximately one-third of human colon cancers (14 of 42 primary tumors and 13 of 38 cell lines).[24] In addition, exogenous *REST* has been shown to suppress the growth of the colon cancer cells that lack *REST* expression, suggesting that REST actually plays a role in the tumor suppression *in vitro*. Although REST-mediated cellular transformation is proposed to be associated with the PI3K pathway, the precise mechanism(s) underlying the involvement of *REST* in colon carcinogenesis remain unclear. In particular, there is no *in vivo* evidence that establishes the function of *Rest* in tumor suppression.

In the present study, we examined the effect of genetic ablation of *Rest* during colon carcinogenesis *in vivo*. We herein show that genetic deletion of *Rest* results in derepression of the Rest-targeted neuronal genes in the colonic crypts, however, *Rest* ablation does not promote mouse colon carcinogenesis.

Materials and Methods

Animals. All animal experiments were approved by the Animal Research Committee of the Graduate School of Medicine, Gifu University (Gifu, Japan). In a previous study, homozygous *Rest* knockout (KO) mice showed embryonic lethality around E10.5, with a growth retardation phenotype.[25] In the present study, in order to investigate the effect of *Rest* deletion on colon carcinogenesis *in vivo*, we used mice expressing conditional knockout alleles of *Rest*.[26] In the *Rest* conditional mice, the endogenous *Rest* loci were replaced by the conditional KO alleles carrying the floxed last exon, which encodes the CoRest binding site that is essential for the generation of the silencing complex.[27] An *ires-Gfp* sequence was inserted into the 3′-UTR of the *Rest* gene to monitor the transcription of the modified allele ($Rest^{2lox}$ allele). The $Rest^{2lox}$ allele was recombined into the $Rest^{1lox}$ allele in the presence of Cre recombinase. Despite the presence of the remaining exons 1–3 of the $Rest^{1lox}$ allele, altered *Rest* transcripts were not detected in $Rest^{1lox/1lox}$ mouse embryonic stem cells,[26] thus suggesting the 1lox allele to be equivalent to the conventional KO allele.

$Apc^{Min/+}$ mice, doxycycline-inducible *Cre* mice, and intestinal epithelium-specific *Cre*-expressing (*Fabp-Cre*) mice were described previously.[26,28,29] Doxycycline-inducible *Cre* mice harbor two transgenes, *Rosa26-M2rtTA* and *Col1A1-tetO-Cre*.[26] The experimental mice were obtained by breeding.

Experimental procedures. We tested the effect of *Rest* ablation in mouse colon carcinogenesis in two independent experiments (Fig. 1). The first experiment (protocol 1) was a chemically-induced colon carcinogenesis model using doxycycline-inducible *Cre*-expressing mice. The other experiment (protocol 2) used the $Apc^{Min/+}$ mouse colon carcinogenesis model combined with the *Fabp-Cre* mouse. In protocol 1, Cre recombinase was induced by doxycycline treatment after carcinogen exposure, mimicking when the *Rest* gene is lost after the initiation phase of carcinogenesis. In contrast, in protocol 2,

[5]To whom correspondence should be addressed.
E-mail: y-yamada@cira.kyoto-u.ac.jp

doi: 10.1111/j.1349-7006.2011.02006.x

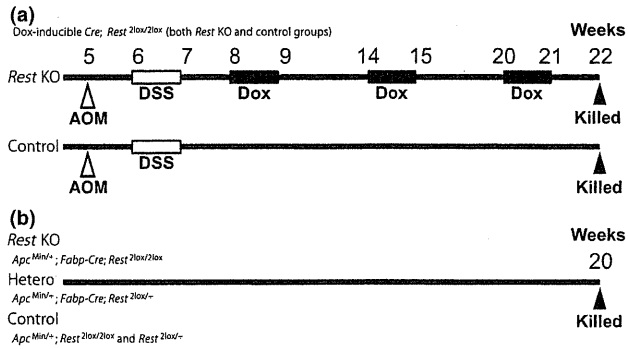

Fig. 1. Schematic drawing of the experimental protocols. The two experiments are different in terms of the timing of the *Rest* recombination. (a) Protocol 1 (*Rest* ablation at the post-initiation phase). (b) Protocol 2 (*Rest* ablation at the pre-initiation phase). Black arrowheads, mice killed; black bars, doxycycline (Dox); white arrowheads, azoxymethane (AOM); white bars, dextran sodium sulfate (DSS). KO, knockout.

Cre-mediated genetic recombination in the intestinal epithelia started before the completion of intestinal morphogenesis, thereby mimicking when the *Rest* recombination occurs before the initiation of carcinogenesis.

In protocol 1, doxycycline-inducible *Cre*; $Rest^{2lox/2lox}$ mice were separated into a *Rest* KO group ($n = 27$) and a control group ($n = 11$). Five-week-old mice were given a single i.p. injection of azoxymethane (15 mg/kg body weight; Wako, Osaka, Japan), a colon-specific carcinogen. One week later, the mice were fed dextran sodium sulfate (20 mg/mL; Wako), a potent tumor promoter for colon tumorigenesis, in their drinking water for 1 week. The mice in the *Rest* KO group were fed 2 mg/mL doxycycline (Sigma, St. Louis, MO, USA) in their drinking water, supplemented with 10 mg/mL sucrose three times per week (at weeks 8, 14, and 20), whereas mice in the control group were fed tap water throughout the experiment. All mice were killed at 22 weeks of age.

In protocol 2, intestine-specific *Rest* KO mice ($Apc^{Min/+}$; *Fabp-Cre*$^+$; $Rest^{2lox/2lox}$ mice, $n = 23$), heterozygous *Rest* KO mice ($Apc^{Min/+}$; *Fabp-Cre*$^+$; $Rest^{2lox/+}$ mice, $n = 32$), and control mice ($Apc^{Min/+}$; *Fabp-Cre*$^-$; $Rest^{2lox/2lox}$ mice and $Apc^{Min/+}$; *Fabp-Cre*$^-$; $Rest^{2lox/+}$ mice, $n = 26$) were examined for the development of colon tumors. All mice were housed in rooms without any chemical treatment during the experiment and were killed at 20 weeks of age.

In both protocols, the colons were cut open longitudinally, then washed with PBS. Visible tumors (larger than 0.5 mm in their maximum diameters) on the colon mucosa were counted, and their maximum diameters were measured. Tumor samples were fixed in 10% buffered formalin for 24 h and embedded in paraffin. Sections were stained with H&E, then serial sections were used for the immunohistochemical analysis. Immunostaining was carried out using an avidin–biotin immunoperoxidase assay. The primary antibodies used in the immunostaining were anti-β-catenin (1:1000 dilution; BD Biosciences, San Diego, CA, USA), anti-chromogranin A (1:1000 dilution; Dako, Carpinteria, CA, USA), and anti-Ki-67 (1:100 dilution; Dako).

Crypt isolation. In order to examine the effect of *Rest* ablation in the colonic epithelium, we carried out crypt isolation to exclude the contaminating stromal cells in the colonic mucosa, as described previously.[29] The removed colon was cut into three equal segments. The distal segment was used for crypt isolation.

Confirmation of *Rest* recombination. To examine the recombination status of the conditional *Rest* allele in the colon, we carried out a Southern blot analysis of the *Rest* loci. Total DNA was extracted from isolated intestinal crypts of doxycycline-inducible *Rest* knockout mice at the indicated time intervals (Fig. 2a). DNA samples (10 μg each) were digested with MfeI (Bio-Rad, Hercules, CA, USA). The digested DNA samples were electrophoresed, transferred onto nylon membranes, and hybridized with a DIG probe against the *Rest* loci in PerfectHyb (Toyobo, Osaka, Japan).[26] Signals were detected by chemiluminescence with LAS-4000 (Fujifilm, Tokyo, Japan). We also carried out a PCR-based analysis to examine the recombination of the *Rest* gene in colon tumors. DNA was isolated from formalin-fixed paraffin-embedding blocks using the Pinpoint Slide DNA Isolation System (Zymo Research, Orange, CA, USA). The PCR was carried out using primers specific for mouse floxed *Rest*. The primers for the $Rest^{2lox}$ allele were forward (F) (5′-CCCTTATGGGTGCAAGTGTT-3′) and reverse (R) (5′-GGGGGACAAAGCCACTCTA-3′). The primers for $Rest^{1lox}$ allele were F (5′-GGGTGCAAGTGTTCTCTTGTCT-3′) and R (5′-CAAGTAACTAAAAATTAGGAACTACCG-3′).

Real-time PCR analysis. Total RNA was extracted from the isolated intestinal crypts as described previously (Fig. 2a), and from the colon tumors of $Apc^{Min/+}$ mice using the RNeasy Mini kit (Qiagen, Valencia, CA, USA). Total RNA (0.5 μg each) was reverse transcribed using Superscript III Reverse Transcriptase (Invitrogen, Carlsbad, CA, USA).

Quantitative real-time PCR was carried out with the Thermal Cycler Dice Real Time System Single (Takara, Kyoto, Japan) using the SYBR Green (Takara) method. The primer sequences used in the quantitative real-time PCR analyses for *Bdnf*, *Tubb3*, and *Rest* were obtained from PrimerBank (http://pga.mgh.harvard.edu/primerbank/). The primers for β-*actin* were F (5′-CATCCGTAAAGACCTCTATGCCAAC-3′) and R (5′-ATGGAGCCACCGATCCACA-3′). The primers for *Gfp* were F (5′-ACCAGCAGAACACCCCCATC-3′) and R (5′-AGCTCGTCCATGCCGAGAGT-3′). The primers for *Syt4* were F (5′-TGCTTTTGGCCTCGTCTTCA-3′) and R (5′-GCGGTTTTACCCTTCACTTCAC-3′).

Statistical analysis. Statistical significance was evaluated using either Student's *t*-test or Welch's *t*-test for paired samples. The results of experiments are presented as the mean ± SEM. $P < 0.05$ was considered to indicate a significant difference.

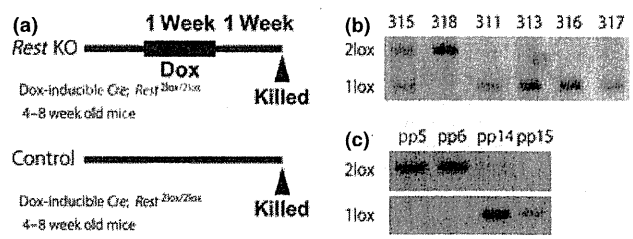

Fig. 2. Genetic recombination of the *Rest* alleles. (a) Doxycycline (Dox)-mediated recombination of *Rest* in protocol 1. A schematic drawing of the experiment. *Rest* conditional knockout (KO) mice with Dox-inducible *Cre* alleles at 4–8 weeks old were treated with 0.2% Dox in their drinking water for 1 week (black bar). Black arrowheads, mice killed. (b) In the Southern blot analysis, in contrast to the control crypts (non-Dox-treated crypts; 315, 318), most of the 2lox alleles in the Dox-treated colonic crypts (311, 313, 316, 317) recombined into 1lox KO alleles. In some cases, the control crypts also contained 1lox alleles (315), probably due to the leaky expression of the *Cre* recombinase. (c) *Rest* recombination in colon tumors in protocol 2. We carried out a PCR-based analysis for *Rest* recombination using colon tumor sections in protocol 2. We could confirm the 1lox KO alleles in five out of six tumors in the *Rest* conditional KO mice with the *Fabp-Cre* allele (pp14 and pp15). However, no recombined *Rest* alleles were observed in any of the nine tumors examined from control mice without the *Fabp-Cre* allele (pp5 and pp6).

doi: 10.1111/j.1349-7006.2011.02006.x

Results

Cre expression induces genetic ablation of _Rest_ in colonic mucosa. In order to examine the efficiency of *Rest* recombination in protocol 1, we carried out a Southern blot analysis using genomic DNA from isolated colonic crypts of doxycycline-inducible *Cre*; $Rest^{2lox/2lox}$ mice (Fig. 2a). The Southern blot analysis revealed that the majority of the $Rest^{2lox}$ alleles in the colonic crypts were recombined into $Rest^{1lox}$ alleles in doxycycline-treated mice (the $Rest^{1lox}$ allele was confirmed in seven out of eight colonic crypts). However, partial recombination of the *Rest* allele was also observed in some cases in the non-treated group (5 out of 13 colonic crypts), probably due to the leaky expression of the *Cre* transgene (Fig. 2b).

In protocol 2, *Rest* recombination was examined using a PCR assay with genomic DNA from formalin-fixed paraffin-embedding specimens of *Fabp-Cre*$^+$; $Rest^{2lox/2lox}$ mice. The recombined *Rest* gene ($Rest^{1lox}$ allele) was only detected in mice containing the *Fabp-Cre* allele, and the $Rest^{2lox}$ allele was also detected in these mice, indicating partial recombination, which is consistent with a previous experiment showing a recombination efficiency of approximately 50% in the colonic crypts by the *Fabp-Cre* allele (Fig. 2c).[28] These results indicate that genetic ablation of *Rest* was induced successfully in the colons of two independent *Cre*-expressing mouse models. In both protocol 1 and 2, despite the presence of the $Rest^{1lox}$ allele, the mice were healthy, and no detectable difference was observed in the histological analyses in comparison to the control mice.

Transcript levels of _Rest_ and Rest-targeted genes in colonic mucosa. We next examined the expression levels of *Rest* in colonic tumors of $Apc^{Min/+}$ mice. The quantitative real-time PCR analysis revealed that *Rest* expression is not different between the colon tumors and non-neoplastic normal mucosa, suggesting that loss of *Rest* is not involved in the colon tumorigenesis of $Apc^{Min/+}$ mice (Fig. 3a). In order to elucidate the effect of genetic ablation of *Rest* in the colonic mucosa, we measured the mRNA expression levels of the *Rest* gene and Rest-targeted genes in the isolated colonic crypts of doxycycline-inducible *Cre*; $Rest^{2lox/2lox}$ mice by quantitative real-time PCR analysis (Fig. 2a). Consistent with the genetic recombination observed in the Southern blot analysis, the expression of *Rest* in the colonic crypts was significantly decreased in the doxycycline-treated mice in comparison with the non-treated mice (Fig. 3b). In line with the decreased expression of the *Rest* gene, the expression of *Gfp* was also downregulated in the doxycycline-treated crypts (Fig. 3c). In contrast, the expression of *Syt4*, *Bdnf*, and *Tubb3*, which are known to be Rest-targeted genes, were significantly upregulated in the doxycycline-treated crypts (Fig. 3d). These results indicate that the genetic recombination of *Rest* results in the rapid derepression of the Rest-targeted genes, suggesting that *Rest* plays a role in the repression of neuronal genes in the colonic crypts.

Macroscopic analysis of colon tumor development. Macroscopically, polypoid tumors were observed in colonic mucosa of mice during both experiments. In protocol 1, genetic recombination into the $Rest^{1lox}$ allele was only confirmed in *Cre*-induced tumors ($n = 4$). In protocol 2, the recombined *Rest* allele ($Rest^{1lox}$ allele) was detectable in the majority of *Rest* KO tumors (5 out of 6 tumors), whereas all control tumors ($n = 9$) retained non-recombined *Rest* alleles ($Rest^{2lox/2lox}$) (Fig. 2c). In protocol 1, the multiplicity of colon tumors was 0.37 ± 0.14/mouse in the *Rest* KO mice and 0.18 ± 0.18/mouse in control mice (Fig. 4a). In protocol 2, the multiplicity and the maximum diameter of colon tumors were 4.96 ± 0.57/mouse and 3.31 ± 0.12 mm in the *Rest* KO mice, 4.81 ± 0.51/mouse and 3.37 ± 0.12 mm in the *Rest* heterozygous mice, and 4.35 ± 0.71/mouse and 3.68 ± 0.15 mm in the control mice, respectively (Fig. 4b,c). No macroscopic tumors were observed

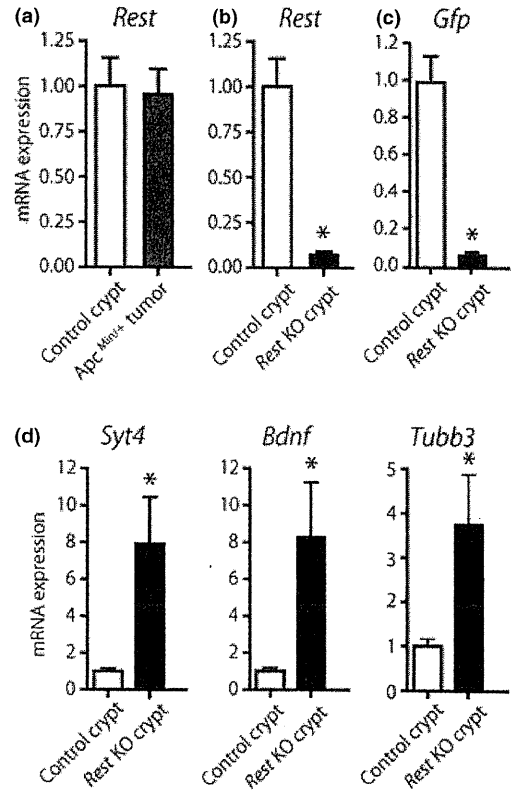

Fig. 3. Transcriptional levels of *Rest* and Rest-targeted neuronal genes in the colon mucosa. (a) $Apc^{Min/+}$ colonic tumors with wild-type *Rest* alleles had nearly the same *Rest* expression level as non-neoplastic crypts. (b–d) Expression levels of *Rest* (b) and *Gfp* (c) were downregulated after the *Rest* ablation in colonic crypts, whereas the expression levels of the Rest-targeted genes (d), *Syt4*, *Bdnf*, and *Tubb3* were significantly upregulated. The mRNA expression levels were analyzed by quantitative real-time PCR and were normalized to the β-actin levels. Data are presented as the mean ± SEM of 13 independent samples. *$P < 0.05$.

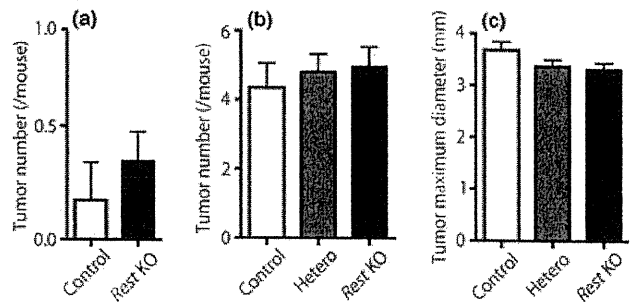

Fig. 4. Macroscopic analysis of colon tumor development. (a) The number of macroscopic tumors in protocol 1. (b,c) The number of macroscopic tumors (b) and the size of tumors (c) in protocol 2. Data are presented as the mean ± SEM.

in the intestine-specific *Rest* KO mice without the Apc^{Min} allele ($Apc^{+/+}$; *Fabp-Cre*$^+$; $Rest^{2lox/2lox}$ mice, $n = 4$). Furthermore, a lack of colon tumor development in *Fabp-Cre*$^+$; $Rest^{2lox/2lox}$ mice was also confirmed in the mice older than 12 months (data not shown), thus suggesting that *Rest* ablation alone is not sufficient to initiate colon tumorigenesis.

Collectively, the multiplicity of colon tumors in the *Rest* KO mice was slightly higher than that in the control mice, but the difference between the *Rest* KO and control mice was not

significantly different (protocol 1: *Rest* KO *vs.* control, $P = 0.46$; protocol 2: *Rest* KO *vs.* control, $P = 0.51$). In addition, no statistically significant difference was observed in the size of the colon tumors, although there was a tendency for the tumor size to correlate with the expression of *Rest* (protocol 2: *Rest* KO *vs.* control, $P = 0.054$).

Histological and immunohistochemical analyses of colon tumors. Colon tumors were processed for histological examinations. As *Rest* recombination occurs partially by the *Fabp-Cre* transgene in protocol 2, the genetic status of *Rest* was determined in each tumor by PCR using primers specific for the $Rest^{2lox}$ and $Rest^{1lox}$ alleles. Regardless of the *Rest* recombination, the histological analysis revealed that all colon tumors consisted of tubular dysplastic glands. There were no detectable histological differences between the colon tumors of *Rest* KO and control mice in either protocol (Fig. 5a).

We further analyzed these tumors by immunostaining for β-catenin, Ki-67, and chromogranin A. The accumulation of β-catenin protein is a critical event that occurs during colon carcinogenesis. Indeed, in the present study, the accumulation of β-catenin was observed in the dysplastic glands in the colonic tumors. However, the β-catenin immunostaining showed no detectable difference between colon tumors in the *Rest* KO and control mice in either protocol (Fig. 5a).

We also carried out Ki-67 immunostaining to compare the proliferative activities of tumor cells with different genetic status of *Rest*. We counted Ki-67 immunopositive tumor cells out of 1000 randomly selected colonic tumor cells from *Rest* KO and control mice, and calculated the ratio of Ki-67 positive tumor cells. The Ki-67 positive cell ratios in the colon tumors of *Rest* KO and control mice were 27.6 ± 3.39% ($n = 5$) and 31.4 ± 4.84% ($n = 5$) in protocol 1 ($P = 0.53$), and 44.2 ± 3.00% ($n = 10$) and 41.2 ± 2.53% ($n = 11$) in protocol 2 ($P = 0.45$), respectively (Table 1).

Rest has been shown to be a master negative regulator of neuronal differentiation. Indeed, we confirmed that genetic ablation of *Rest* leads to the derepression of neuronal gene expression. Therefore, we next examined the enteroendocrine cell differentiation of the intestinal cells after loss of *Rest* expression. Chromogranin A immunostaining was used to assess the endocrine differentiation of both non-neoplastic and tumor cells in the colon. Chromogranin A immunostaining showed no detectable differences related to the *Rest* recombination in both non-neoplastic and tumor cells (Fig. 5b). The positive cell ratios for chromogranin A in *Rest* KO and control tumors was 0.28 ± 0.08% ($n = 5$) and 0.10 ± 0.07% ($n = 5$) in protocol 1 ($P = 0.12$), and 0.07 ± 0.02% ($n = 10$) and 0.12 ± 0.02% ($n = 11$) in protocol 2 ($P = 0.17$), respectively (Table 1).

Discussion

Colon carcinogenesis is a multistage process involving genetic and epigenetic alterations of various tumor suppressor genes and oncogenes. Our previous studies identified two distinct stages of colon tumorigenesis in $Apc^{Min/+}$ mice (microadenomas and macroscopic tumors).[30] The formation of microadenomas is accompanied by the activation of the canonical Wnt pathway through the genetic loss of the *Apc* gene, leading to the accumulation of β-catenin. Recent evidence suggests that DNA methylation is closely associated with the progression of microadenomas into macroscopic tumors.[28,31–33] Although the identity of the target genes of DNA methylation involved in colon tumorigenesis remain unclear, these findings suggest that the progression of colonic tumors in $Apc^{Min/+}$ mice requires synchronous alternations in the expression of multiple genes due to global changes of epigenetic modifications.

REST, a novel candidate tumor suppressor gene in colon carcinogenesis, maintains transcriptional silencing of various genes by recruiting multiple co-factors, including Co-Rest,[27] HDAC and Sin3 complex,[34–36] histone H3 K9 methyltransferase G9a,[37] histone H3 K4 demethylase LSD1,[38] and methyl DNA binding protein MeCP2.[39] Previous experiments indicated

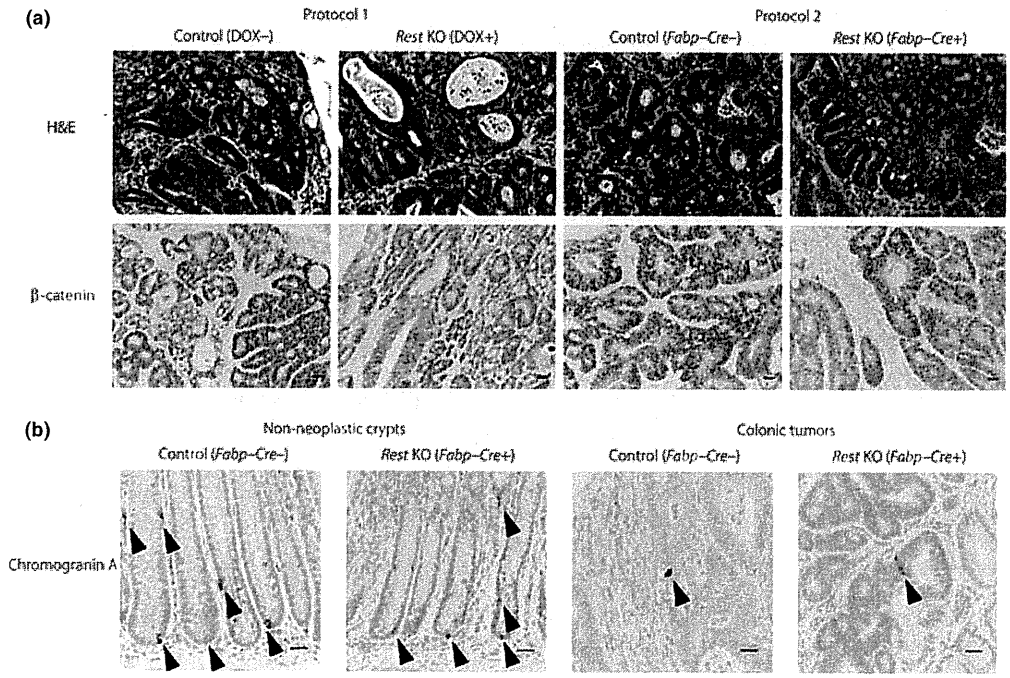

Fig. 5. Histological and immunohistochemical analyses of colonic tumors. (a) There was no detectable difference in the H&E staining (upper panels) and β-catenin immunostaining (lower panels) between the *Rest* knockout (KO) and control tumors in either protocol. (b) Chromogranin A immunostaining of colonic non-neoplastic and tumor cells. Black arrowheads, chromogranin A immunopositive cells, *Rest* KO: $Apc^{Min/+}$; *Fabp-Cre*$^{+}$; $Rest^{2lox/2lox}$ mice, control: $Apc^{Min/+}$; $Rest^{2lox/2lox}$ mice. Dox, doxycycline. Scale bars = 20 μm.

doi: 10.1111/j.1349-7006.2011.02006.x

Table 1. Ki-67 and chromogranin A positive tumor cell ratio in colon tumors of *Rest* knockout (KO) and control mice

		Ki-67 (%)	Chromogranin A (%)
Protocol 1	*Rest* KO	27.6 ± 3.39	0.28 ± 0.08
	Control	31.4 ± 4.84	0.10 ± 0.07
Protocol 2	*Rest* KO	44.2 ± 3.00	0.07 ± 0.02
	Control	41.2 ± 2.53	0.12 ± 0.02

Protocol 1, chemically-induced colon carcinogenesis model using doxycycline-inducible *Cre*-expressing mice. Protocol 2, $Apc^{Min/+}$ mouse colon carcinogenesis model combined with *Fabp-Cre* mouse.

thousands of REST-targeted genes in embryonic stem cells and neuronal progenitor cells.[40] REST is thus suggested to alter the chromatin structure in conjunction with its co-factors, while also regulating the transcription of the REST-targeted genes through histone modification, chromatin remodeling, and genomic methylation. Given the fact that DNA methylation, one of the most important epigenetic modifications, plays a critical role in the transition from microadenomas to macroscopic tumors in the colon of $Apc^{Min/+}$ mice, we hypothesized that the global changes in epigenetic modifications caused by *Rest* ablation might affect murine colon tumorigenesis.

In this study, we confirmed that the genetic ablation of *Rest* leads to the decreased expression of *Rest* and increased expression of Rest-targeted genes, suggesting that Rest represses the Rest-targeted genes in the colonic crypts. However, *Rest* ablation at both the pre-initiation and post-initiation phases of colon tumorigenesis showed no significant effect on tumor development in the colon. These findings indicate that loss of *Rest* expression by itself does not promote the development of colon tumors in mice. It is possible that *Rest* deletion alone might not be sufficient for the active changes of epigenetic modifications to induce the progression of colon tumorigenesis.

Rest has been regarded as a master negative regulator of neuronal differentiation in non-neuronal cells. Indeed, a targeted mutation of *Rest* in mice caused derepression of neuron-specific genes in a subset of non-neuronal tissues. Human colonic carcinoma expressing neuroendocrine genes (also called neuroendocrine carcinoma, NEC) is a highly aggressive carcinoma that comprises approximately 0.6% of colonic carcinomas.[41] Importantly, most neuroendocrine genes expressed in NEC are targets of the REST-repressing complex. Considering that the genetic deletion of *Rest* leads to the upregulation of neuronal genes in non-neuronal cells, we hypothesized that *Rest* deletion would induce neuronal differentiation in colonic tumors, thus leading to a NEC-like phenotype. In fact, previous studies have revealed that carcinomas with *REST* dysfunction frequently showed neuroendocrine characteristics.[8,12–16] However, in the present study, colon tumors lacking the *Rest* gene did not show the NEC-like histology. In addition, an increase in chromogranin A-positive cells, which is usually observed in NEC, was not detectable in the *Rest*-deleted tumors. Our results suggest that, although *Rest* ablation leads to the increased mRNA expression of neuronal genes, *Rest* ablation alone is not sufficient to induce neuronal differentiation in the colon. As the incidence of NEC is extremely rare compared to the relatively high incidence of *REST* deletion in colorectal cancer,[24,41] it is still possible that *REST* inactivation, in conjunction with additional genetic and/or epigenetic alterations, may be involved in the development of NEC. In this context, it would be interesting to examine the genetic status of *REST* in NEC in future studies.

In summary, we have shown that the genetic ablation of *Rest* does not affect the development of colon tumors in mice. These findings suggest that other genetic and/or epigenetic alterations might therefore be required to exert the tumor-promoting effect of *Rest* ablation during multistage tumorigenesis of the colon.

Acknowledgments

We thank Kyoko Takahashi, Ayako Suga, and Yoshitaka Kinjo for their technical assistance. This study was supported by grants from the Ministry of Education, Culture, Sports, Science and Technology of Japan, and grants from PRESTO, and from the Ministry of Health, Labour and Welfare of Japan.

Disclosure Statement

The authors have no conflict of interest to declare.

References

1 Chong JA, Tapia-Ramirez J, Kim S *et al.* REST: a mammalian silencer protein that restricts sodium channel gene expression to neurons. *Cell* 1995; **80**: 949–57.
2 Schoenherr CJ, Anderson DJ. The neuron-restrictive silencer factor (NRSF): a coordinate repressor of multiple neuron-specific genes. *Science* 1995; **267**: 1360–3.
3 Ballas N, Grunseich C, Lu DD, Speh JC, Mandel G. REST and its corepressors mediate plasticity of neuronal gene chromatin throughout neurogenesis. *Cell* 2005; **121**: 645–57.
4 Jones FS, Meech R. Knockout of REST/NRSF shows that the protein is a potent repressor of neuronally expressed genes in non-neural tissues. *Bioessays* 1999; **21**: 372–6.
5 Coulson JM. Transcriptional regulation: cancer, neurons and the REST. *Curr Biol* 2005; **15**: 665–8.
6 Majumder S. REST in good times and bad: roles in tumor suppressor and oncogenic activities. *Cell Cycle* 2006; **5**: 1929–35.
7 Weissman AM. How much REST is enough? *Cancer Cell* 2008; **13**: 381–3.
8 Tawadros T, Martin D, Abderrahmani A, Leisinger HJ, Waeber G, Haefliger JA. IB1/JIP-1 controls JNK activation and increased during prostatic LNCaP cells neuroendocrine differentiation. *Cell Signal* 2005; **17**: 929–39.
9 Reddy BY, Greco SJ, Patel PS, Trzaska KA, Rameshwar P. RE-1-silencing transcription factor shows tumor-suppressor functions and negatively regulates the oncogenic TAC1 in breast cancer cells. *Proc Natl Acad Sci USA* 2009; **106**: 4408–13.
10 Wagoner MP, Gunsalus KT, Schoenike B, Richardson AL, Friedl A, Roopra A. The transcription factor REST is lost in aggressive breast cancer. *PLoS Genet* 2010; **6**: e1000979.
11 Lv H, Pan G, Zheng G *et al.* Expression and functions of the repressor element 1 (RE-1)-silencing transcription factor (REST) in breast cancer. *J Cell Biochem* 2010; **110**: 968–74.
12 Coulson JM, Edgson JL, Woll PJ, Quinn JP. A splice variant of the neuron-restrictive silencer factor repressor is expressed in small cell lung cancer: a potential role in derepression of neuroendocrine genes and a useful clinical marker. *Cancer Res* 2000; **60**: 1840–4.
13 Gurrola-Diaz C, Lacroix J, Dihlmann S, Becker CM, von Knebel Doeberitz M. Reduced expression of the neuron restrictive silencer factor permits transcription of glycine receptor alpha1 subunit in small-cell lung cancer cells. *Oncogene* 2003; **22**: 5636–45.
14 Neumann SB, Seitz R, Gorzella A, Heister A, Doeberitz MK, Becker CM. Relaxation of glycine receptor and onconeural gene transcription control in NRSF deficient small cell lung cancer cell lines. *Brain Res Mol Brain Res* 2004; **120**: 173–81.
15 Moss AC, Jacobson GM, Walker LE, Blake NW, Marshall E, Coulson JM. SCG3 transcript in peripheral blood is a prognostic biomarker for REST-deficient small cell lung cancer. *Clin Cancer Res* 2009; **15**: 274–83.
16 Kreisler A, Strissel PL, Strick R, Neumann SB, Schumacher U, Becker CM. Regulation of the NRSF/REST gene by methylation and CREB affects the cellular phenotype of small-cell lung cancer. *Oncogene* 2010; **29**: 5828–38.
17 Lawinger P, Venugopal R, Guo ZS *et al.* The neuronal repressor REST/NRSF is an essential regulator in medulloblastoma cells. *Nat Med* 2000; **6**: 826–31.
18 Fuller GN, Su X, Price RE *et al.* Many human medulloblastoma tumors overexpress repressor element-1 silencing transcription (REST)/neuron-restrictive silencer factor, which can be functionally countered by REST-VP16. *Mol Cancer Ther* 2005; **4**: 343–9.

19 Su X, Gopalakrishnan V, Stearns D *et al.* Abnormal expression of REST/NRSF and Myc in neural stem/progenitor cells causes cerebellar tumors by blocking neuronal differentiation. *Mol Cell Biol* 2006; **26**: 1666–78.
20 Nishimura E, Sasaki K, Maruyama K, Tsukada T, Yamaguchi K. Decrease in neuron-restrictive silencer factor (NRSF) mRNA levels during differentiation of cultured neuroblastoma cells. *Neurosci Lett* 1996; **211**: 101–4.
21 Palm K, Metsis M, Timmusk T. Neuron-specific splicing of zinc finger transcription factor REST/NRSF/XBR is frequent in neuroblastomas and conserved in human, mouse and rat. *Brain Res Mol Brain Res* 1999; **72**: 30–9.
22 Donev RM, Gray LC, Sivasankar B, Hughes TR, Van den Berg CW, Morgan BP. Modulation of CD59 expression by restrictive silencer factor-derived peptides in cancer immunotherapy for neuroblastoma. *Cancer Res* 2008; **68**: 5979–87.
23 Lietz M, Cicchetti P, Thiel G. Inverse expression pattern of REST and synapsin I in human neuroblastoma cells. *Biol Chem* 1998; **379**: 1301–4.
24 Westbrook TF, Martin ES, Schlabach MR *et al.* A genetic screen for candidate tumor suppressors identifies REST. *Cell* 2005; **121**: 837–48.
25 Chen ZF, Paquette AJ, Anderson DJ. NRSF/REST is required *in vivo* for repression of multiple neuronal target genes during embryogenesis. *Nat Genet* 1998; **20**: 136–42.
26 Yamada Y, Aoki H, Kunisada T, Hara A. Rest promotes the early differentiation of mouse ESCs but is not required for their maintenance. *Cell Stem Cell* 2010; **6**: 10–5.
27 Andres ME, Burger C, Peral-Rubio MJ *et al.* CoREST: a functional corepressor required for regulation of neural-specific gene expression. *Proc Natl Acad Sci USA* 1999; **96**: 9873–8.
28 Lin H, Yamada Y, Nguyen S *et al.* Suppression of intestinal neoplasia by deletion of Dnmt3b. *Mol Cell Biol* 2006; **26**: 2976–83.
29 Sakai H, Yamada Y, Shimizu M, Saito K, Moriwaki H, Hara A. Genetic ablation of Tnfalpha demonstrates no detectable suppressive effect on inflammation-related mouse colon tumorigenesis. *Chem Biol Interact* 2010; **184**: 423–30.
30 Yamada Y, Mori H. Multistep carcinogenesis of the colon in Apc(Min/+) mouse. *Cancer Sci* 2007; **98**: 6–10.
31 Yamada Y, Jackson-Grusby L, Linhart H *et al.* Opposing effects of DNA hypomethylation on intestinal and liver carcinogenesis. *Proc Natl Acad Sci USA* 2005; **102**: 13580–5.
32 Laird PW, Jackson-Grusby L, Fazeli A *et al.* Suppression of intestinal neoplasia by DNA hypomethylation. *Cell* 1995; **81**: 197–205.
33 Linhart HG, Lin H, Yamada Y *et al.* Dnmt3b promotes tumorigenesis *in vivo* by gene-specific de novo methylation and transcriptional silencing. *Genes Dev* 2007; **21**: 3110–22.
34 Huang Y, Myers SJ, Dingledine R. Transcriptional repression by REST: recruitment of Sin3A and histone deacetylase to neuronal genes. *Nat Neurosci* 1999; **2**: 867–72.
35 Naruse Y, Aoki T, Kojima T, Mori N. Neural restrictive silencer factor recruits mSin3 and histone deacetylase complex to repress neuron-specific target genes. *Proc Natl Acad Sci USA* 1999; **96**: 13691–6.
36 Roopra A, Sharling L, Wood IC *et al.* Transcriptional repression by neuron-restrictive silencer factor is mediated via the Sin3-histone deacetylase complex. *Mol Cell Biol* 2000; **20**: 2147–57.
37 Shi Y, Sawada J, Sui G *et al.* Coordinated histone modifications mediated by a CtBP co-repressor complex. *Nature* 2003; **422**: 735–8.
38 Shi Y, Lan F, Matson C *et al.* Histone demethylation mediated by the nuclear amine oxidase homolog LSD1. *Cell* 2004; **119**: 941–53.
39 Lunyak VV, Burgess R, Prefontaine GG *et al.* Corepressor-dependent silencing of chromosomal regions encoding neuronal genes. *Science* 2002; **298**: 1747–52.
40 Bruce AW, Donaldson IJ, Wood IC *et al.* Genome-wide analysis of repressor element 1 silencing transcription factor/neuron-restrictive silencing factor (REST/NRSF) target genes. *Proc Natl Acad Sci USA* 2004; **101**: 10458–63.
41 Bernick PE, Klimstra DS, Shia J *et al.* Neuroendocrine carcinomas of the colon and rectum. *Dis Colon Rectum* 2004; **47**: 163–9.

doi: 10.1111/j.1349-7006.2011.02006.x

CHEMBIOCHEM

DOI: 10.1002/cbic.201100597

Synthetic Small Molecules for Epigenetic Activation of Pluripotency Genes in Mouse Embryonic Fibroblasts

Ganesh N. Pandian,[a] Ken-ichi Shinohara,[a, b, e] Akimichi Ohtsuki,[b] Yusuke Nakano,[b] Minoshima Masafumi,[b] Toshikazu Bando,[b] Hiroki Nagase,[c, f] Yasuhiro Yamada,[d] Akira Watanabe,[d] Naohiro Terada,[e] Shinsuke Sato,[a] Hironobu Morinaga,[b] and Hiroshi Sugiyama*[a, b]

Considering the essential role of chromatin remodeling in gene regulation, their directed modulation is of increasing importance. To achieve gene activation by epigenetic modification, we synthesized a series of pyrrole–imidazole polyamide conjugates (PIPs) that can bind to predetermined DNA sequences, and attached them with suberoylanilide hydroxamic acid (SAHA), a potent histone deacetylase inhibitor. As histone modification is associated with pluripotency, these new types of conjugates, termed SAHA–PIPs, were screened for their effect on the expression of induced pluripotent stem cell (iPSC) factors. We found certain SAHA–PIPs that could differentially up-regulate the endogenous expression of *Oct-3/4*, *Nanog*, *Sox2*, *Klf4* and *c-Myc*. SAHA and other SAHA–PIPs did not show such induction; this implies a role for PIPs and their sequence specificity in this differential gene activation. Chromatin immunoprecipitation analysis suggested that SAHA–PIP-mediated gene induction proceeds by histone H3 Lys9 and Lys14 acetylation and Lys4 trimethylation, which are epigenetic features associated with transcriptionally active chromatin.

Introduction

N-Methylpyrrole (P) and *N*-methylimidazole (I) hairpin polyamides are programmable synthetic molecules that can precisely recognize each of the four Watson–Crick base pairs. A pairing of I opposite P (I–P) recognizes a G:C base pair, whereas a P–P pair recognizes A:T or T:A.[1] PI polyamides have been widely used to target sequences of biological interest for regulating gene expression due to their high sequence specificity and ability to cross the plasma membrane and nuclear envelope and bind the target chromosomal DNA with an affinity similar to that of a transcription factor.[2–4] Recently, we reported the synthesis of PI polyamide conjugates (PIPs) possessing a suberoylanilide hydroxamic acid (SAHA) moiety, which acts as an effective histone deacetylase (HDAC) inhibitor with a broad spectrum of epigenetic activities. These novel SAHA–PIPs, which were designed to target the promoter region of *p16* tumor suppressor gene in HeLa cells, induced histone H3 Lys9 acetylation.[5] Encouraged with the selective inducing ability of these small molecules, we have synthesized a new library of sequence specific SAHA-PIPs that could cause distinctive up-regulation of endogenous gene expression.

Generation of induced pluripotent stem cells (iPSCs) from somatic fibroblasts by using defined factors could lead to groundbreaking clinical applications; however, the risk of carcinogenesis hampers the clinical translation of this rapidly advancing technology.[6–9] Notwithstanding the recent promising breakthroughs,[10] several hurdles, including the retention of epigenetic memory,[11] need to be overcome before the possible therapeutic use of iPSCs. Since dynamic chromatin structure is connected intimately with the fundamental nature of a cell, chromatin modifiers could establish and maintain pluripotent status in somatic cells.[12] As chromatin modifiers lack selectivity, supplementing them with distinctive recognition through PIPs could pave the way for precise up-regulation of particular gene. In view of this, we have chosen to test our library of SAHA–PIPs by screening for their effect on the endogenous expression of the standard iPSC reprogramming factors

[a] *Dr. G. N. Pandian,[+] Dr. K.-i. Shinohara,[+] S. Sato, Prof. H. Sugiyama*
Institute for Integrated Cell–Material Sciences (iCeMS)
Kyoto University, Yoshida Ushinomiya-cho
Sakyo, Kyoto 606-8501 (Japan)
E-mail: hs@kuchem.kyoto-u.ac.jp

[b] *Dr. K.-i. Shinohara,[+] Dr. A. Ohtsuki, Y. Nakano, Dr. M. Masafumi, Dr. T. Bando, H. Morinaga, Prof. H. Sugiyama*
Department of Science, Graduate School of Science
Kyoto University, Sakyo, Kyoto 606-8502 (Japan)

[c] *Prof. H. Nagase*
Division of Cancer Genetics, Chiba Cancer Center Research Institute
666-2 Nitona-cho, Chuo-ku, Chiba-shi, Chiba 260-8717 (Japan)

[d] *Prof. Y. Yamada, Dr. A. Watanabe*
Center for iPS Cell Research and Application (CiRA)
Kyoto University, Kyoto 606-8507 (Japan)

[e] *Dr. K.-i. Shinohara,[+] Prof. N. Terada*
Department of Pathology, College of Medicine
University of Florida, Gainesville, FL 32610-0275 (USA)

[f] *Prof. H. Nagase*
Division of Cancer Genetics, Department of Advanced Medical Science
Nihon University School of Medicine, Tokyo 173-8610 (Japan)

[+] *These authors contributed equally to this work.*

Supporting information for this article is available on the WWW under http://dx.doi.org/10.1002/cbic.201100597.

(*Oct-3/4*, *Nanog*, *Sox2*, *Klf4* and *c-Myc*) in mouse embryonic fibroblasts (MEF). Herein, we report for the first time, the ability of our programmable DNA-binding small molecules to differentially up-regulate iPSC factor(s) in MEF by inducing histone modifications that are associated with pluripotency.

Results

Synthesis of SAHA–PIPs

To achieve distinct gene activation, we designed 16 types of SAHA–PIPs (**A** to **P**) to specifically target a 6 base pair (bp) sequence based on the binding rule of PI polyamides mentioned before (Figure 1). These hairpin PI polyamides are expected to have high binding affinities (nM order) to specific DNA sequences.[5] A SAHA moiety was conjugated to the N tail with a double β-alanine linker in the hairpin PI polyamides. All SAHA–PIPs had one cationic tertiary amino group at the C tail. PI polyamides possessing a (8-methoxy-8-oxo-octanamido)benzoic acid moiety as a SAHA precursor were synthesized by Fmoc solid-phase synthesis by using an oxime resin, and subsequent 3-(dimethylamino)-1-propylamine treatment. After the preparative reversed-phase column chromatography, each precursor was efficiently converted to a SAHA–PIP (**A** to **P**) by using NH_2OH (50%, *v/v*). After HPLC purification, the structures of **A** to **P** were confirmed by using ESI-ToF MS.

SAHA–PIPs differentially up-regulate endogenous expression of iPSC factors

We screened our library of designed SAHA–PIPs (Figure 1, **A–P**) for their effect on the endogenous expression of reprogramming factors (*Oct-3/4*, *Nanog*, *Sox2*, *Klf4* and *c-Myc*). Endogenous *Oct-3/4* was notably induced by about 3.2-fold with **E** and 2.8-fold with **O**; for *Nanog*, **E** and **O** showed approximately 2.7- and 2.2-fold induction, respectively (Figure 2A and B, bars **E** and **O**). Compounds **J**, **O** and **D** showed about 2.6-, 2.3- and 2.1-fold increase in the expression of *Sox2* (Figure 2C, bar **J**), *Klf4* (Figure 2D, bar **O**) and *c-Myc* (Figure 2E, bar **D**), respectively. It is important to note here that only SAHA showed almost no effect on the expression level of all the five iPSC reprogramming factors; this implicates the PIPs as the cause behind the distinctive gene expression (Figure 2A–E, bar SAHA).

Compounds **D**, **E**, **J** and **O** were chosen as "hit" SAHA–PIPs as they notably induced all five iPSC reprogramming factors. When the cytotoxicity of SAHA–PIPs in MEF cells was evaluated, with **E** as the representative compound, nearly no cytotoxic effect was observed even at 10 μM, whereas SAHA at this concentration reduced cell viability by about 85% (Figure S1A and B in the Supporting Information). Thus, the differential gene expression by SAHA–PIPs is not attributable to cytotoxic effects. Moreover, at a working concentration of 100 nM for either SAHA or SAHA–PIP and DMSO (0.1%), cell viability was not affected. Interestingly, our hit SAHA–PIPs could notably induce the iPSC factors in just 24 h. Recently various small molecules including BIX-01294, Bayk8644, Repsox, HDAC inhibitors

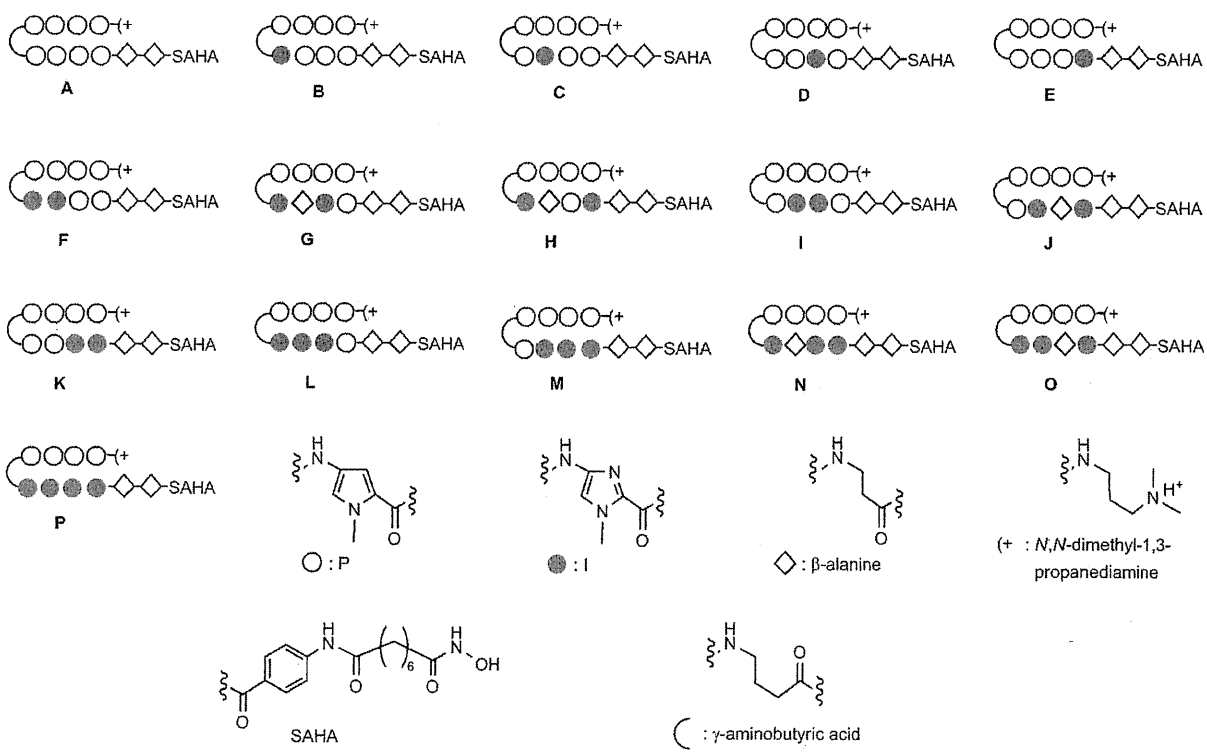

Figure 1. Chemical structures and target sequences (W = A or T) of the synthetic SAHA–pyrrole–imidazole polyamide conjugates **A–P**.

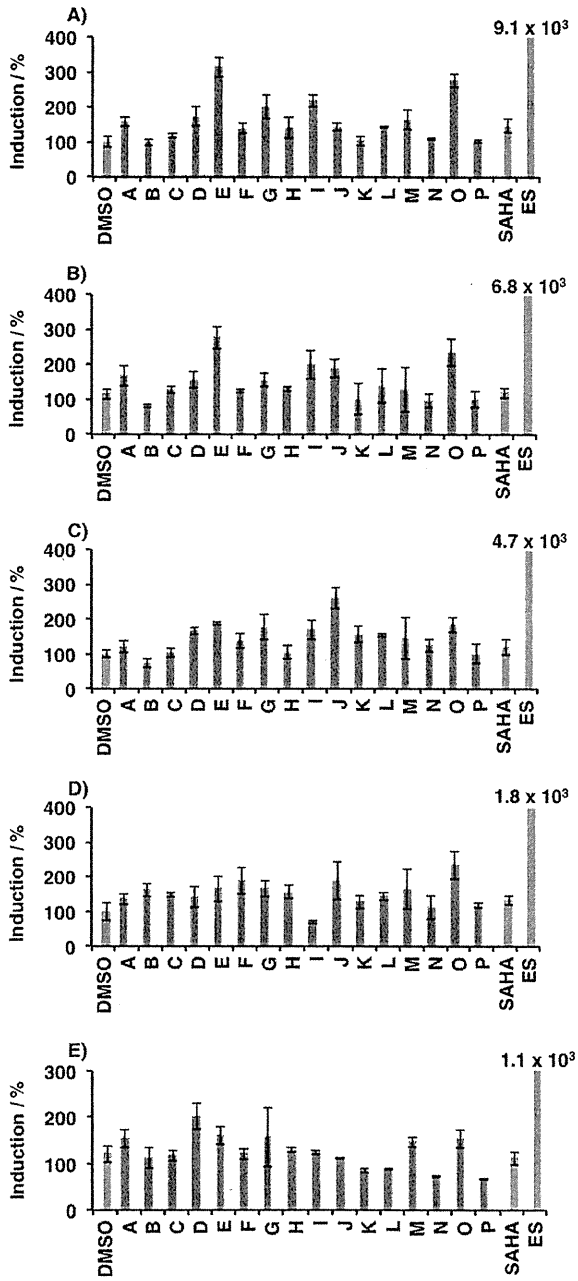

Figure 2. SAHA–PIPs cause differential up-regulation of endogenous genes that contribute to pluripotency. Quantitative RT-PCR analysis of the expression level of the iPSC factors: A) *Oct-3/4*, B) *Nanog*, C) *Sox2*, D) *Klf4*, and E) *c-Myc*. Light gray bars represent the control samples: DMSO and SAHA as the negative controls, and ES cells as the positive control. Dark green bars represent the expression profiles of the endogenous genes with 16 individual SAHA–PIPs (**A** to **P**). Each bar represents mean ± SD from 72-well plates.

(valproic acid and sodium butyrate), pifithrin-α (a p53 inhibitor), 6-bromoindirubin-3′-oxime (BIO) and vitamin C have been shown to improve reprogramming efficiency by inducing the iPSC factors.[13–20] For a comparative study of the effect of these small molecules on the endogenous expression of iPSC factors, they were used individually and in combination with our hit SAHA–PIPs. The combination of selected SAHA–PIPs displayed about a two- to threefold increase in the endogenous expression of all iPSC factors (Figure S2 in the Supporting Information, bar SP), but only a mild effect on induction values was observed when they were combined with small molecules (Figure S2, bar SPSM).

Chromatin immunoprecipitation assay in the promoter region of *Oct-3/4* and *Nanog*

Since the *Oct-3/4* and *Nanog* transcriptional network regulates pluripotency,[21] the promoter region for these two genes were analyzed to evaluate the effect of SAHA–PIPs on the acetylation of histones H3 and H4. Hit SAHA–PIPs, **E** and **O**, were chosen for this study as both notably induced the endogenous expression of *Oct-3/4* and *Nanog*. SAHA–PIP **B** and SAHA alone were used as controls to corroborate the sequence specificity. MEF cells treated with effectors were immunoprecipitated against antibodies for either acetylated histone H4 or H3 at Lys9 or Lys14 (H4Kac, H3K9ac and H3K14ac), as described in the Supporting Information. In the case of *Oct-3/4*, **E** and **O** showed about five- to sixfold increase in the acetylation of H4K and H3K9 (Figure 3A, H4Kac and H3K9ac); acetylation of

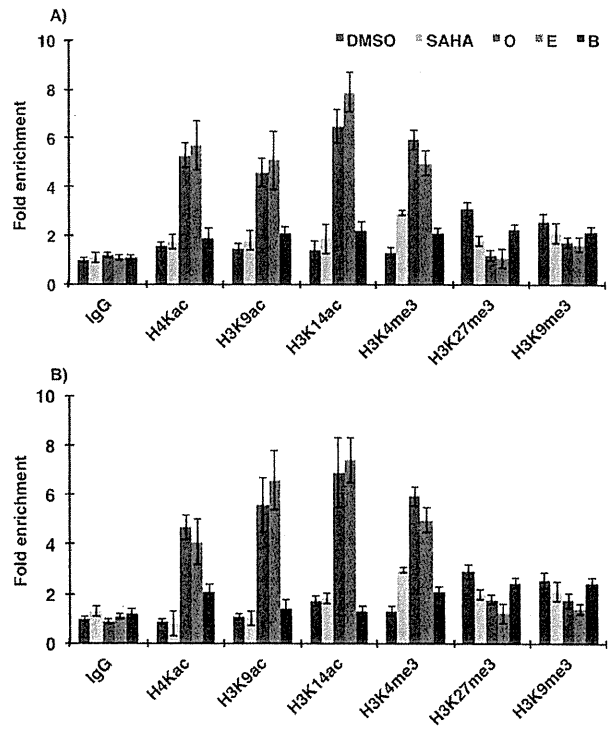

Figure 3. SAHA–PIP inducible histone modifications in the promoter region of *Oct-3/4* and *Nanog*. MEF cells were treated for 24 h with SAHA–PIP **O**, **E**, **B** and SAHA only (100 nM). DMSO (0.1%) treated cells were used as the control. After immunoprecipitation with H4Kac, H3K9ac, H3K14ac, H3K4me3 H3K27me3 and H3K9me3 antibodies, the amount of promoter sequence of: A) *Oct-3/4* and B) *Nanog*, in the co-precipitated DNA samples was determined by quantitative PCR. Enrichment fold in acetylation was calculated by normalizing the data against input DNA, and by normalizing the enrichment with IgG antibody. Each bar represents mean ± SD from 24 wells.

H3K14 was enriched by about six- to sevenfold (Figure 3A, H3K14ac).

As our selected SAHA–PIPs notably alter the endogenous expression of pluripotency genes, MEF cells treated with the above-mentioned effectors were also immunoprecipitated with antibodies against histone H3 Lys4 trimethylation (H3K4me3), an epigenetic marker associated with active chromatin. As a control, MEF cells were also immunoprecipitated with antibodies against histone H3, Lys9 and Lys27 trimethylation (H3K9me3 and H3K27me3), which are epigenetic modifications associated with repressed chromatin. Intriguingly, **E** and **O** also showed about a four- to fivefold enrichment with H3K4me3 and mild reduction with H3K27me3 and H3K9me3, when compared with DMSO treated cells (Figure 3A, H3K4me3, H3K9me3 and H3K27me3).

A similar pattern was observed in the *Nanog* promoter region; **E** and **O** showed enrichment in the markers for activation and a mild reduction in those for repression (Figure 3B, bars **E** and **O**). Only SAHA and **B** showed a relatively mild effect in both (Figure 3A and B, bars SAHA and **B**), which signifies the role of PIPs in the acetylation-mediated active chromatin modifications and induction of endogenous *Oct-3/4* and *Nanog*.

Region specific chromatin modification in *Nanog*

To evaluate whether the effect of our hit SAHA–PIP(s) is specific to a certain site, the epigenetic markers around the *Nanog* region were analyzed as this also contains the *oct–sox* binding sites. The activation markers (H4Kac, H3K9ac, H3K14ac and H3K4me3) were analyzed along with H3K9me3 and H3K27me3, by following the same method as mentioned above with the primers designed around the transcription start site (TSS) and for the regions that are 2 kbp downstream and 1 kbp upstream or downstream the transcription start site candidate (Figure 4A). Compounds **O** and **E** showed notable acetylation of about four- to fivefold enrichment in H3K9, and about a six- to sevenfold enrichment in H3K14 and H4K with the primer pairs designed around the transcription start site (Figure 4B–D, bars **O** and **E** in TSS 1 and TSS 2). It is important to note that no notable increase in acetylation of H4K, H3K9 and H3K14 was observed with the primers selected for the regions 2 kbp downstream and 1 kbp upstream or downstream the transcription start site candidate (Figure 4B–D, bars TSS −2, TSS −1 and TSS +1).

Likewise, **O** and **E** showed considerable enrichment in the trimethylation level of H3K4 along with reduction in H3K27 and H3K9, predominantly in TSS 2, while no such effect was observed in TSS −2, TSS −1 and TSS +1 (Figure 4E and Figure S3 in the Supporting Information). Lack of such enrichment with **B** and SAHA clearly indicates that the hit SAHA–PIPs could distinctly enrich the activation markers in the promoter and transcription regions of *Nanog*.

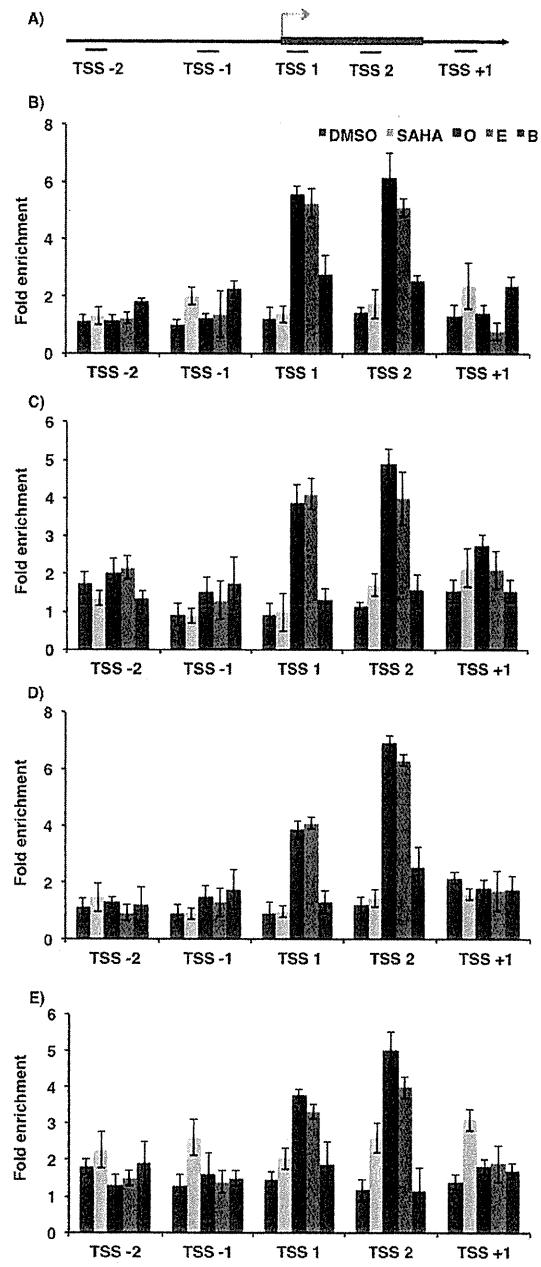

Figure 4. Effect of SAHA–PIPs on the epigenetic modification in the *Nanog* promoter region. A) Location of the transcription start site in the 4 kbp promoter region of *Nanog*. A colored bar indicates the site around the transcription region. Green arrow mark indicates the TSS (transcription start site). TSS 1 and TSS 2 represent the transcription start site candidates 1 and 2, respectively. TSS −1 and TSS −2 represent the regions located 1 and 2 kbp upstream of TSS 1. TSS +1 represents the region located 1 kbp downstream of TSS 1. MEF cells were treated for 24 h with SAHA–PIP **O**, **E**, **B** and SAHA only (100 nM). DMSO (0.1%) treated cells were used as control. After immunoprecipitation with H4Kac, H3K9ac, H3K14ac and H3K4me3 antibodies, the co-precipitated DNA samples were analyzed by quantitative PCR by using the primer pairs designed as described in the Supporting Information. Expression profiles of: B) H4Kac, C) H3K9ac, D) H3K14ac, and E) H3K4me3 are shown. Enrichment fold in acetylation and methylation was calculated by normalizing the data against input DNA and by normalizing the enrichment with IgG antibody as 1. Each bar represents mean ± SD from 24 wells.

Discussion

We have explored the prospect of developing PIPs as artificial genetic switches to recognize DNA sequences or local structures of interest, and thus created a bottom-up approach to control the expression of a specific gene of interest. The demand for the means to induce pluripotency in somatic cells has increased, and several groups have already identified chemicals that can replace one, two or even three reprogramming factors during iPSCs generation.[13–15] It is generally accepted that aberrant reprogramming with a smaller number of factors can render iPSCs refractory to differentiation.[22] Thus, establishing ways to precisely generate each iPSC clone is important for viable therapeutic applications. This could also be achieved by sequence specific up-regulation of the gene(s) and factors contributing to the generation of iPSCs. Recent progress in iPSC technology suggests that *Oct-3/4* and *Nanog* are indispensable in regulating pluripotency and self-renewal of stem cells, and thus, chemicals that activate the endogenous *Oct-3/4* and *Nanog* genes could have potential applications in establishing and maintaining pluripotency in somatic cells. As shown in Figure 2 and Figure S2 in the Supporting Information, our selected SAHA–PIPs, **E** and **O**, can notably induce the expression levels of both *Oct-3/4* and *Nanog* in just 24 h when compared to other small molecules, with the added advantage of possible sequence-specific chromatin remodeling.

Pluripotent cells have dynamic and open chromatin structures when compared with that of somatic cells. Chromatin immunoprecipitation analysis suggests that only selected SAHA-PIPs (**O** and **E**) induced enrichment of activation markers (H4Kac, H3K9ac, H3K14ac and H3K4me3) with a moderate reduction in markers for repression (H3K9me3 and H3K27me3), whereas **B**, SAHA or DMSO did not show such an effect (Figure 3). Furthermore, this enrichment for activation markers and slight reduction in markers for repression, was observed only in the TSS region of *Nanog* (Figure 4 and Figure S3 in the Supporting Information). Analysis of the number of matching sites in the *Nanog* gene revealed that **E** had a significant number of binding sites, about six-times higher than **B** around the promoter and transcription region, but not in the other regions; this corroborates the sequence specificity. Although our SAHA–PIPs were expected to cause acetylation, enrichment of trimethylation in H3K4 is possible, as HDAC inhibitors are also known to stimulate H3K4me3 through transcriptional repression of histone H3 Lys4 demethylases.[23] It is generally accepted that the state of DNA methylation is closely associated with transcriptional regulation in iPSCs, and interestingly, we have shown that PI polyamides can bind methylated $^{5'}$-CpG-$^{3'}$ sequences with threefold higher binding affinities than the unmethylated $^{5'}$-CpG-$^{3'}$ sequence.[24]

Post-translational modifications to histones affect chromatin structure and function and result in altered gene expression and changes in stem cell behavior, while aberrant gene expression and altered epigenomic patterns are major features of cancer. Hence, our approach opens new vistas of opportunities to modulate the epigenetic environment of certain genes, and thus could be developed for applications in both cancer and stem cell biology.

In summary, while screening for the effects of our library of SAHA–PIPs, we found that some of them could distinctly up-regulate iPSC factor(s) in MEF by histone modifications that are associated with pluripotency. Although the induction effect of iPSC reprogramming factors by our selected SAHA–PIPs is notable even with 24 h incubation, it is still low when compared with that of embryonic stem (ES) cells (Figure 2). Nevertheless, PI polyamides are versatile artificial molecules owing to their ease and flexibility of design, automation-driven solid-phase synthesis, cell permeability and the presence of flexible sites for covalent attachment to other molecules.[25–27] We have also shown 10 bp recognition by alkylating DNA with PI 1-(chloromethyl)-5-hydroxy-1,2-dihydro-3*H*-benz[e]indole (*seco*-CBI) conjugates.[28] Accordingly, it is possible to expand our library of PI polyamides and increase the sequence specificity to improve the expression level of pluripotent factor(s) that could eventually lead to sequence-specific induction of pluripotent stem cells. However, several hurdles need to be overcome to achieve this goal and to develop our molecules to generate iPSCs.

Experimental Section

General preparation of PI polyamide by Fmoc solid-phase synthesis: Synthesis and characterization of 4-(8-methoxy-8-oxo-octanamido)benzoic acid was carried out as mentioned before.[5] All machine-assisted PI polyamide syntheses were performed on a PSSM-8 peptide synthesizer (Shimadzu, Kyoto, Japan) with a computer-assisted operation system at oxime resin (80 mg, 0.5 mmol g^{-1}, 200–400 mesh) by using Fmoc chemistry. Reaction steps in the synthesis cycle were as follows: deblocking steps for 2×4 min, piperidine (20%) in DMF; coupling step for 60 min, corresponding carboxylic acids, HCTU (88 mg), DIEA (36 μL), DMF; washing steps for 5×1 min, with DMF. Coupling reagents in each step were prepared in DMF: Fmoc-P-COOH (77 mg), Fmoc-I-COOH (77 mg), Fmoc-PI-COOH (103 mg), Fmoc-β-COOH (66 mg), Fmoc-γ-COOH (69 mg), 4-(8-methoxy-8-oxo-octanamido)benzoic acid (65 mg). All other couplings were carried out with single couple cycles and were stirred by bubbling N_2 gas. Typically, Fmoc-P-oxime resin (80 mg, 0.04 mmol) was swollen in DMF (1 mL) in a plastic reaction vessel (2.5 mL) for 30 min. Plastic centrifuge tubes (2 mL) with loading Fmoc-monomers with HCTU in DMF (1 mL) were placed in order of position. The synthesis was then started, controlled by computer by using the established program. All lines were washed with DMF after solution transfers. After the completion of the synthesis on the peptide synthesizer, the resin was washed with a mixture of methanol and CH_2Cl_2 (2 mL) and dried in a desiccator at room temperature, in vacuo.

Synthesis of SAHA–PIP O: A dried sample resin was cleaved with *N,N*-dimethylaminopropylamine (0.6 mL) for 5 h at 45 °C. The reaction mixture was filtered, recrystallized from Et_2O, and was purified by HPLC in ammonium formate (AF, 50 mM) containing 0–100% CH_3CN over a linear gradient for 20 min at a flow of 1 mL min^{-1} at 40 °C and the absorbance was detected at 256 nm; 4-(8-methoxy-8-oxo-octanamido)benzoyl PIP **O** was obtained as a yellow powder. This precursor of SAHA–PIP **O** (about 10 mg) was dissolved in DMF (0.5 mL) and was added to an aqueous solution of 50% (*v/v*) NH_2OH (0.5 mL). The reaction mixture was stirred for 8 h at room temperature. Subsequently, the hydroxylamine was quenched with

acetic acid (0.5 mL) at 0 °C. The mixture was purified by HPLC in AF (50 mM) containing CH_3CN (0–100%) over a linear gradient for 20 min at a flow of 1 mL min^{-1} at 40 °C, and the absorbance was detected at 254 nm; SAHA–PIP **O** was obtained as a white powder (1.9 mg, 4%). ^{1}H NMR (600 MHz, [D_6]DMSO): δ = 10.40 (s, 1H; NH), 10.36 (s, 1H; NH), 10.32 (s, 1H; NH), 10.09 (s, 2H; NH), 9.93 (s, 2H; NH), 9.82 (s, 1H; NH), 9.37 (s, 1H; NH), 8.34 (s, 1H; NH), 8.23 (s, 1H; NH), 8.16 (s, 1H; NH), 8.01 (s, 1H; NH), 7.98 (s, 1H; NH), 7.75 (d, J = 8.9 Hz, 2H; CH), 7.63 (d, J = 8.9 Hz, 2H; CH), 7.51 (s, 1H; CH), 7.49 (s, 1H; CH), 7.40 (s, 1H; CH), 7.22 (s, 2H; CH), 7.17 (s, H; CH), 7.15 (s, H; CH), 7.08 (s, 2H; CH), 6.95 (s, H; CH), 6.88 (s, H; CH), 3.96 (s, 6H; NCH_3), 3.91 (s, 3H; NCH_3), 3.85 (s, 3H; NCH_3), 3.85 (s, 3H; NCH_3), 3.83 (s, 3H; NCH_3), 3.81 (s, 3H; NCH_3), 3.25–3.37 (m, 8H; CH_2), 3.32 (m, 2H; CH_2), 3.28 (m, 2H; CH_2), 3.25 (m, 2H; CH_2), 3.07 (brs, 2H; CH_2), 2.79 (s, 6H; NCH_3), 2.61 (s, 2H; CH_2), 2.61 (s, 2H; CH_2), 2.59 (m, 2H; CH_2), 2.39 (m, 2H; CH_2), 2.34 (m, 2H; CH_2), 2.30 (m, 2H; CH_2), 2.27 (m, 2H; CH_2), 1.93 (m, 2H; CH_2), 1.84 (m, 2H; CH_2), 1.80 (m, 2H; CH_2),1.56 (m, 2H; CH_2),1.48 (m, 2H; CH_2), 1.27 (brs, 2H; CH_2); ESI-ToF MS *m/z* calcd for $C_{72}H_{95}N_{25}O_{15}$: 774.87 $[M+2H]^{2+}$, found 774.87.

The stock solution of purified PI polyamide was prepared by dissolving the compound in DMSO. A procedure similar to that used for the preparation of compound **O** was adopted to prepare all the other SAHA–PIPs as shown below.

*SAHA–PIP **D** (SAHA–ββPIPPγPPPPDp):* White powder (2.5 mg, 5%), ESI-ToF MS *m/z* calcd for $C_{77}H_{98}N_{24}O_{15}$ $[M+2H]^{2+}$ 799.38, found 799.42.

*SAHA–PIP **E** (SAHA–ββIPPPγPPPPDp):* White powder (1.4 mg, 3%), ESI-ToF MS *m/z* calcd for $C_{77}H_{98}N_{24}O_{15}$ $[M+2H]^{2+}$ 799.38, found 799.41.

*SAHA–PIP **J** (SAHA–ββIβIPγPPPPDp):* White powder (2.5 mg, 6%), ESI-ToF MS *m/z* calcd for $C_{73}H_{96}N_{24}O_{15}$ $[M+2H]^{2+}$ 774.38, found 774.43.

*SAHA–PIPs (**A, B, C, F, G, H, I, K, L, M, N, P**):* SAHA–PIP **A** (SAHA–ββPPPPγPPPPDp), SAHA–PIP **B** (SAHA–ββPPPIγPPPPDp), SAHA–PIP **C** (SAHA–ββPPIPγPPPPDp), SAHA–PIP **F** (SAHA–ββPPIIγPPPPDp), SAHA–PIP **G** (SAHA–ββPIβIγPPPPDp), SAHA–PIP **H** (SAHA–ββIPβIγPPPPDp), SAHA–PIP **I** (SAHA–ββPIIPγPPPPDp), SAHA–PIP **J** (SAHA–ββIβIPγPPPPDp), SAHA–PIP **K** (SAHA–ββIIPPγPPPPDp), SAHA–PIP **L** (SAHA–ββPIIIγPPPPDp), SAHA–PIP **M** (SAHA–ββIIIPγPPPPDp), SAHA–PIP **N** (SAHA–ββIIβIγPPPPDp) and SAHA–PIP **P** (SAHA–ββIIIIγPPPPDp).

The structures of the PI polyamide conjugates **A**–**P** are shown in the Figure 1. The stock solution of purified PI polyamide was prepared by dissolving the compound in DMSO.

Treatment of MEF cells with SAHA–PIPs and optimization: MEF cells in the sixth passage were trypsinized for 5 min at 37 °C, and were resuspended in fresh DMEM medium to give a concentration of 2×10^5 cells per mL in a 35 mm plate. After overnight incubation for attachment, the medium was replaced with fresh DMEM (2 mL) containing each individual SAHA–PIP solution. All plates were incubated in a 5% CO_2 humidified atmosphere at 37 °C for 24 h. Incubation time and concentration of the SAHA–PIPs were standardized based on initial optimization experiments with varied incubation time (24, 48 and 72 h) and SAHA–PIP concentrations (50, 100, 200, 500 nM, and 1 and 10 μM). No significant effect on the expression profile of the iPSC reprogramming factors was observed by varying the incubation time. When the effect of concentration of SAHA–PIPs was studied with **E**, **O** and **B** as representatives, **E** and **O** (100 nM) showed the maximum of threefold induction; increase in the concentration of the SAHA–PIP conjugate did not have a significant effect on the expression profile of iPSC reprogramming factors. Based on these optimization studies, SAHA–PIPs were treated at a final concentration (100 nM in 0.1% DMSO). Mouse ES cells, DMSO (0.1%) and SAHA (100 nM) treated cells were used as controls.

Details regarding cell culture, analysis of gene expression, chromatin immunoprecipitation and other protocols are given in the Supporting Information.

Acknowledgements

This research was supported by the Ministry of Education, Culture, Sports, Science and Technology of Japan (MEXT), administrated by the Japan Society for the Promotion of Science.

Keywords: biomimetic synthesis · chromatin remodeling · DNA recognition · genetic switches · pluripotency genes

[1] S. White, J. W. Szewczyk, J. M. Turner, E. E. Baird, P. B. Dervan, *Nature* **1998**, *391*, 468–471.
[2] J. M. Gottesfeld, L. Neely, J. W. Trauger, E. E. Baird, P. B. Dervan, *Nature* **1997**, *387*, 202–205.
[3] T. Bando, H. Sugiyama, *Acc. Chem. Res.* **2006**, *39*, 935–944.
[4] S. Nishijima, K. Shinohara, T. Bando, M. Minoshima, G. Kashiwazaki, H. Sugiyama, *Bioorg. Med. Chem.* **2010**, *18*, 978–983.
[5] A. Ohtsuki, M. T. Kimura, M. Minoshima, T. Suzuki, M. Ikeda, T. Bando, H. Nagase, K. Shinohara, H. Sugiyama, *Tetrahedron Lett.* **2009**, *50*, 7288–7292.
[6] K. Takahashi, S. Yamanaka, *Cell* **2006**, *126*, 663–676.
[7] K. Takahashi, K. Tanabe, M. Ohnuki, M. Narita, T. Ichisaka, K. Tomoda, S. Yamanaka, *Cell* **2007**, *131*, 861–872.
[8] I. H. Park, N. Arora, H. Huo, N. Maherali, T. Ahfeldt, A. Shimamura, M. W. Lensch, C. Cowan, K. Hochedlinger, G. Q. Daley, *Cell* **2008**, *134*, 877–886.
[9] O. Tsuji, K. Miura, Y. Okada, K. Fujiyoshi, M. Mukaino, N. Nagoshi, K. Kitamura, G. Kumagai, M. Nishino, S. Tomisato, H. Higashi, T. Nagai, H. Katoh, K. Kohda, Y. Matsuzaki, M. Yuzaki, E. Ikeda, Y. Toyama, M. Nakamura, S. Yamanaka, H. Okano, *Proc. Natl. Acad. Sci. USA* **2010**, *107*, 12704–12709.
[10] M. Maekawa, K. Yamaguchi, T. Nakamura, R. Shibukawa, I. Kodanaka, T. Ichisaka, Y. Kawamura, H. Mochizuki, N. Goshima, S. Yamanaka, *Nature* **2011**, *474*, 225–229.
[11] K. Kim, A. Doi, B. Wen, K. Ng, R. Zhao, P. Cahan, J. Kim, M. J. Aryee, H. Ji, L. I. Ehrlich, A. Yabuuchi, A. Takeuchi, K. C. Cunniff, H. Hongguang, S. McKinney-Freeman, O. Naveiras, T. J. Yoon, R. A. Irizarry, N. Jung, J. Seita, J. Hanna, P. Murakami, R. Jaenisch, R. Weissleder, S. H. Orkin, I. L. Weissman, A. P. Feinberg, G. Q. Daley, *Nature* **2010**, *467*, 285–290.
[12] P. Delgado-Olguin, F. Recillas-Targa, *Briefings Funct. Genomics Proteomics* **2011**, *10*, 37–49.
[13] J. K. Ichida, J. Blanchard, K. Lam, E. Y. Son, J. E. Chung, D. Egli, K. M. Loh, A. C. Carter, F. P. Di Giorgio, K. Koszka, D. Huangfu, H. Akutsu, D. R. Liu, L. L. Rubin, K. Eggan, *Cell Stem Cell* **2009**, *5*, 491–503.
[14] Y. Shi, C. Desponts, J. T. Do, H. S. Hahm, H. R. Scholer, S. Ding, *Cell Stem Cell* **2008**, *3*, 568–574.
[15] Y. Li, Q. Zhang, X. Yin, W. Yang, Y. Du, P. Hou, J. Ge, C. Liu, W. Zhang, X. Zhang, Y. Wu, H. Li, K. Liu, C. Wu, Z. Song, Y. Zhao, Y. Shi, H. Deng, *Cell Res.* **2011**, *21*, 196–204.
[16] J. Silva, O. Barrandon, J. Nichols, J. Kawaguchi, T. W. Theunissen, A. Smith, *PLoS Biol.* **2008**, *6*, e253.
[17] D. Huangfu, R. Maehr, W. Guo, A. Eijkelenboom, M. Snitow, A. E. Chen, D. A. Melton, *Nat. Biotechnol.* **2008**, *26*, 795–797.
[18] P. Mali, B. K. Chou, J. Yen, Z. Ye, J. Zou, S. Dowey, R. A. Brodsky, J. E. Ohm, W. Yu, S. B. Baylin, K. Yusa, A. Bradley, D. J. Meyers, C. Mukherjee, P. A. Cole, L. Cheng, *Stem Cells* **2010**, *28*, 713–720.

